NI

NASA Technical Memorandum 83194

(NASA-TM-83194) BUCKLING LOADS FOR STIFFENED PANELS SUBJECTED TO COMBINED LONGITUDINAL COMPRESSION AND SHEAR LOADINGS: RESULTS OBTAINED WITH PASCO, EAL, AND STAGS COMPUTER (NASA) 65 p HC A04/MF A01 CSCL 20K G3/39

N81-33498

Unclas 27679

BUCKLING LOADS FOR STIFFENED PANELS SUBJECTED TO COMBINED LONGITUDINAL COMPRESSION AND SHEAR LOADINGS: RESULTS OBTAINED WITH PASCO, EAL, AND STAGS COMPUTER PROGRAMS

W. JEFFERSON STROUD, WILLIAM H. GREENE, AND MELVIN S. ANDERSON

OCTOBER 1981

National Aeronautics and Space Administration

Langley Research Center
Hampton, Virginia 23665

CONTENTS

BUCKLING LOADS FOR STIFFENED PANELS SUBJECTED TO COMBINED LONGITUDINAL COMPRESSION AND SHEAR LOADINGS: RESULTS OBTAINED WITH PASCO, EAL, AND STAGS COMPUTER PROGRAMS

W. Jefferson Stroud, William H. Greene, and Melvin S. Anderson

SUMMARY

The buckling analyses used in PASCO are summarized with emphasis placed on the shear buckling analyses. PASCO analyses include the basic VIPASA analysis, which is essentially exact for longitudinal and transverse loads, and a smeared orthotropic solution that was added in an attempt to alleviate a shortcoming in the VIPASA analysis--underestimation of overall shear buckling loads. Buckling results are then presented for six stiffened panels loaded by combinations of longitudinal compression and shear. The buckling results were obtained with the PASCO (VIPASA and smeared orthotropic solutions), EAL, and STAGS computer programs. The EAL and STAGS solutions were obtained with a fine finite element mesh and, therefore, provide benchmark calculations for the entire range of combinations of longitudinal compression and shear loadings considered.

INTRODUCTION

Whereas buckling analysis procedures that are both fast and accurate have been developed for stiffened panels subjected to longitudinal (N_x) and transverse (N_y) loadings (for example, VIPASA, refs. 1-3, and BUCLASP, ref. 4), no such procedure has been developed for analyzing stiffened panels subjected to loadings involving shear (N_{xy}). VIPASA comes very close to meeting both objectives; however, when the loading involves shear, VIPASA underestimates the buckling load for the overall mode--that is, the mode for thich the buckling half-wavelength in the direction of the stiffeners is equal to the panel length. VIPASA is generally accurate for loadings involving shear when the buckling

half-wavelength in the direction of the stiffeners is less than one third the panel length.

Shear buckling analysis procedures in current use include the following modeling approaches: Stiffeners modeled as linked plates with infinite panel length (VIPASA, ref. 1); hinges along plate element connections for local buckling and smeared stiffnesses for overall buckling (for example, ref. 5); approximations using discrete EI and GJ stiffeners; and general purpose finite difference and finite element approaches (for example, EAL, refs. 6-7, and STAGS, refs. 8-9). All of these approaches have shortcomings. The shortcoming of the approach used in VIPASA is mentioned in the previous paragraph and is discussed in this report. When stiffnesses are smeared, local deformations that contribute to the overall buckling mode are lost. Local deformations are also lost when the stiffeners are modeled as EI and GJ stiffeners. Finite difference and finite element approaches can provide high accuracy by using small meshes; however, to obtain accurate results the computation costs are high.

Because VIPASA is the buckling analysis in PASCO, an alternate solution approach for predicting overall shear buckling was explored and incorporated in PASCO. That approach, which is referred to herein as the adjusted analysis, is based on smeared orthotropic stiffnesses. The purpose of this report is to present shear buckling results obtained using PASCO (includes both VIPASA and smeared orthotropic solutions), EAL, and STAGS to help evaluate the shear buckling analyses in PASCO. These results also provide accurate benchmark calculations to evaluate other analysis procedures.

SYMBOLS

Values are given in both SI and U.S. Customary Units. The calculations were made in U.S. Customary Units.

E	Young's modulus
E_1, E_2	Young's modulus of composite material in fiber direction and and transverse to fiber direction, respectively
E_{12}	shear modulus of composite material in coordinate system defined by fiber direction
F	scalar factor that relates input loading to eigenvalue (see eq. 2)
$F_{d,0}$	value of F for discrete stiffeners with stiffeners in x-direction. This is the standard VIPASA solution
$F_{d,90}$	value of F obtained from equation (3)
$F_{s,0}$	value of F for smeared stiffnesses with stiffeners in x-direction
$F_{s,90}$	value of F for smeared stiffnesses with stiffeners in y-direction
L	panel length
N_x	applied longitudinal compressive loading per unit width of panel (see fig. 1)
N_{xy}	applied shear loading per unit width of panel (see fig. 1)
N_y	applied transverse loading per unit width of panel (see fig. 1)
u, v, w	buckling displacements
W	panel width
X, Y, Z	overall panel axes
x, y, z	coordinates in longitudinal, transverse, and lateral directions, respectively
X, Y_ℓ, Z_ℓ	local element axes
x, y_ℓ, z_ℓ	local coordinates for each element making up a panel

ϵ_x	strain in x-direction
λ	buckling half-wavelength
μ	Poisson's ratio
μ_1, μ_2	Poisson's ratios of composite material in coordinate system defined by fiber direction, $\mu_1 = \mu_2 E_1/E_2$

BUCKLING ANALYSES IN PASCO FOR LOADINGS INVOLVING SHEAR

Abbreviated descriptions of the buckling analyses used in PASCO are presented. Emphasis is placed on the effect of a shear loading. A more complete description is presented in references 1 and 11.

VIPASA Buckling Analysis

Except for special analysis techniques discussed in a subsequent section entitled Adjusted Analysis for Shear, the buckling analysis in PASCO is VIPASA, described in references 1-3, 10-12. VIPASA treats an arbitrary assemblage of plate elements with each plate element i loaded by N_{x_i}, N_{y_i}, and N_{xy_i}. The overall panel coordinate system (X, Y, Z) is shown in figure 1(a); the local plate element coordinate system (X_ℓ, Y_ℓ, Z_ℓ), displacements, loadings, and sign convention are shown in figures 1(b) and 1(c). The buckling analysis connects the individual plate elements and maintains continuity of the buckle pattern across the intersection of neighboring plate elements.

The buckling displacement w assumed in VIPASA for each plate element is

$$w = f_1(y_\ell) \cos\frac{\pi x}{\lambda} - f_2(y_\ell) \sin\frac{\pi x}{\lambda} \qquad (1)$$

Similar expressions are assumed for the inplane displacement u and v. The functions $f_1(y_\ell)$ and $f_2(y_\ell)$ allow various boundary conditions to be prescribed on the lateral edges of the panel. Boundary conditions cannot be prescribed on the ends of the panel.

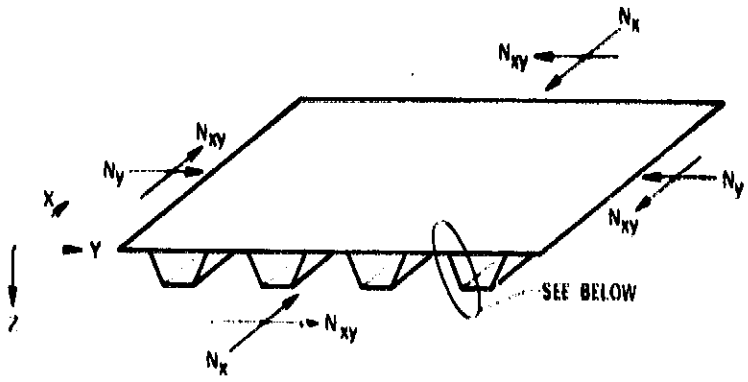

(a) Hat-stiffened panel with applied N_x, N_y, and N_{xy} loading and overall panel coordinate system

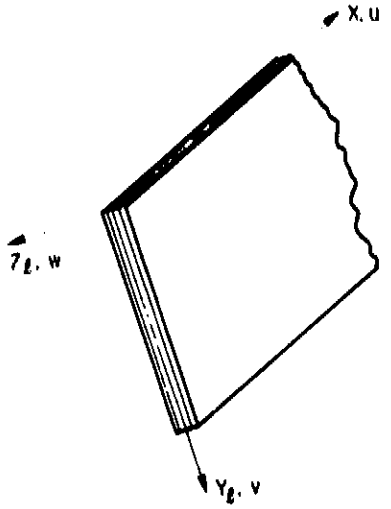

(b) Local plate element coordinate system and displacements.

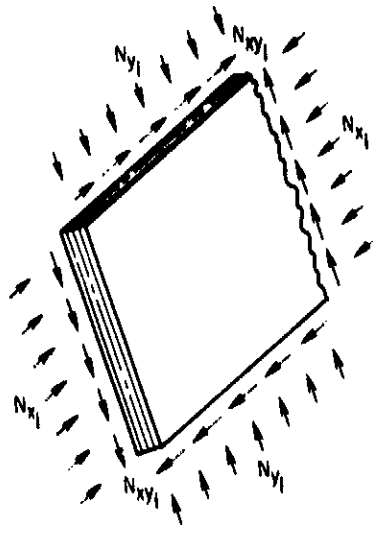

(c) Plate element i with inplane loading. Directions shown are positive for prebuckling loads.

Figure 1.- Overall panel coordinate system and local plate element coordinate system, displacements, loading, and sign convention.

For orthotropic plate elements with no shear loading, $f_2(y_\ell)$ is zero. The solution $f_1(y_\ell) \cos \frac{\pi x}{\lambda}$ provides a series of node lines that are straight, perpendicular to the longitudinal panel axis, and spaced λ apart as shown in figure 2. Along each of these node lines, the buckling displacements satisfy simple support boundary conditions. For values of λ given by $\lambda = L, L/2, L/3, \ldots L/m$, where m is an integer, the nodal pattern shown in figure 2 provides simple support boundary conditions at the ends of a finite, rectangular panel of length L. An example in which $\lambda = L/2$ is shown in figure 3.

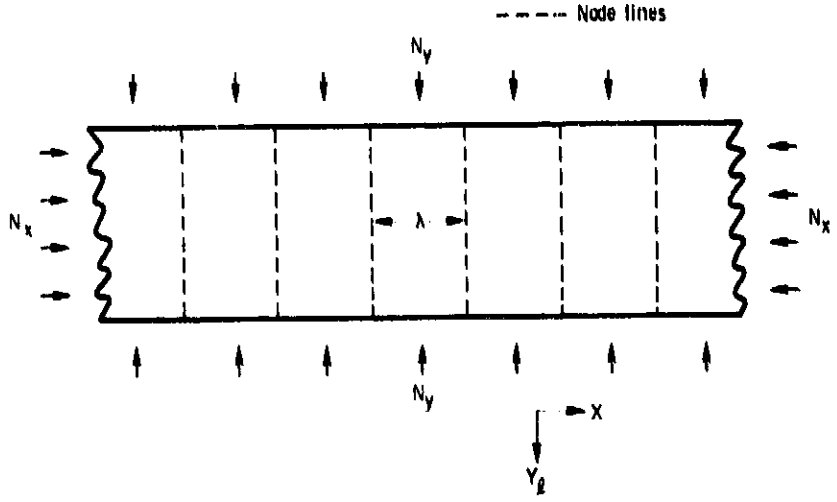

Figure 2.- Node lines produced by $w = f_1(y_\ell) \cos \frac{\pi x}{\lambda}$.

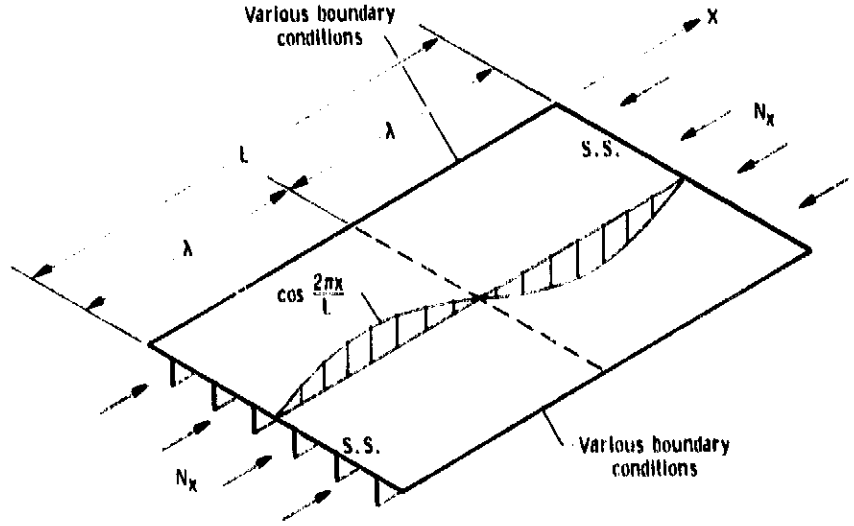

Figure 3.- Buckling of orthotropic panel under longitudinal loading. Mode shown is $\lambda = L/2$.

For anisotropic plate elements and/or plate elements with a shear loading, $f_2(y_\ell)$ is not zero. (Because anisotropy generally has negligible effect for long-wavelength buckling modes and because it is these long-wavelength modes that are troublesome, reference to anisotropy is dropped in the following discussion.) Node lines are skewed and not straight, but the node lines are still spaced λ apart as shown in figure 4. Since node lines cannot coincide with the ends of the rectangular panel, the VIPASA solution for loadings involving shear is accurate only when many buckles form along the panel length, in which case boundary conditions at the ends are not important. An example in which $\lambda = L/4$ is shown in figure 5.

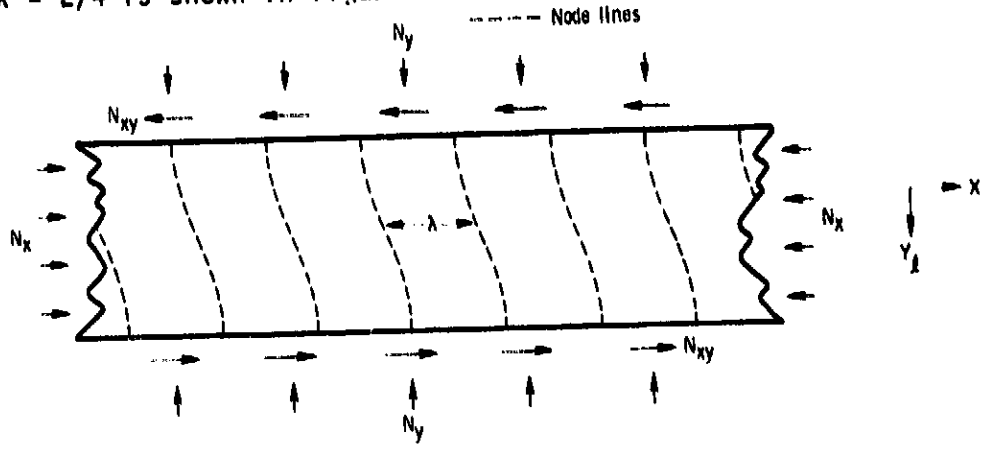

Figure 4.- Node lines produced by $w = f_1(y_\ell) \cos\frac{\pi x}{\lambda} - f_2(y_\ell) \sin\frac{\pi x}{\lambda}$

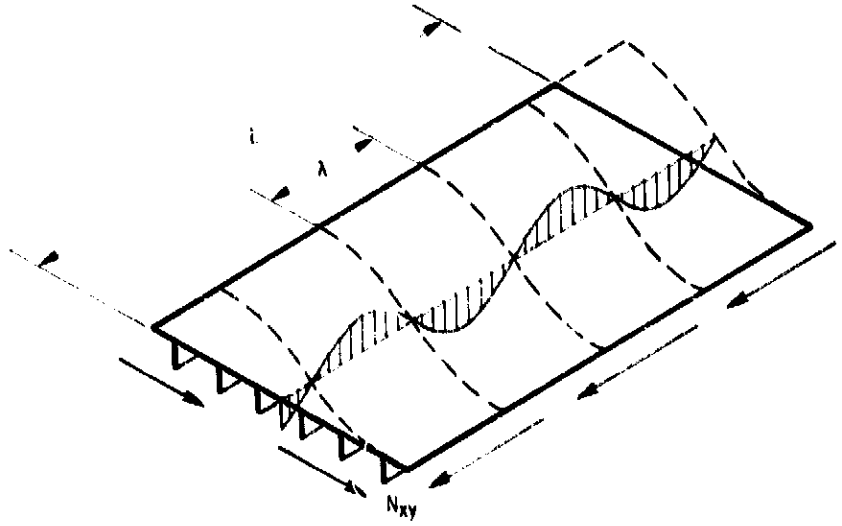

Figure 5.- Buckling of panel under shear loading. Mode shown is $\lambda = L/4$.

As λ approaches L, the VIPASA buckling analysis for a panel loaded by N_{xy} can underestimate the buckling load substantially. One explanation is as follows: As can be seen in figure 5, the skewed nodal lines given by VIPASA in the case of shear do not coincide with the end edges. Forcing node lines (and, therefore, simple support boundary conditions) to coincide with the end edges produces long-wavelength buckling loads that are, in many cases, appreciably higher than those determined by VIPASA.

In summary, for stiffened panels composed of orthotropic plate elements with no shear loading, the VIPASA solution is exact in the sense that it is the exact solution of the plate equations satisfying the Kirchoff-Love hypothesis. However, for stiffened panels having a shear loading the VIPASA solution can be very conservative for the case $\lambda = L$. It is believed that for this case the VIPASA solution provides a lower bound.

Because VIPASA is overly conservative in the case of long-wavelength buckling if a shear load is present, an adjusted shear analysis procedure based on smeared orthotropic stiffnesses has been incorporated in PASCO. This adjusted analysis can be used (at the user's option) for the case $\lambda = L$.

Adjusted Analysis for Shear

In VIPASA, a scalar quantity denoted FACTOR is the unknown in the eigenvalue analysis. In this report, a quantity is introduced that has essentially the same meaning as FACTOR. That quantity is denoted F. The quantities FACTOR and F differ only in that whereas FACTOR is always the solution of an eigenvalue analysis in VIPASA and is identified with the word FACTOR in the VIPASA printout, F may not be the solution of a VIPASA eigenvalue analysis if an adjusted shear analysis is used in PASCO. Otherwise, FACTOR and F are identical. In

this report, the scalar F is defined by

$$F \begin{bmatrix} N_x \\ N_y \\ N_{xy} \end{bmatrix}_{\text{input}} = \begin{bmatrix} N_x \\ N_y \\ N_{xy} \end{bmatrix}_{\text{eigenvalue}} \tag{2}$$

Where N_x, N_y, and N_{xy} are inplane loads. A definition of F which involves additional loads is given in reference 11.

The rationale presented here for the adjusted analysis approach is somewhat different from that presented in reference 11. The objective of the analysis is to solve the shear buckling problem for the finite panel illustrated in figure 6. For buckling half-wavelength λ equal to panel length L, the mathematical model solved by VIPASA and the resulting node lines are similar to those illustrated in figure 7. The panel in figure 7 is infinitely long in the x-direction.

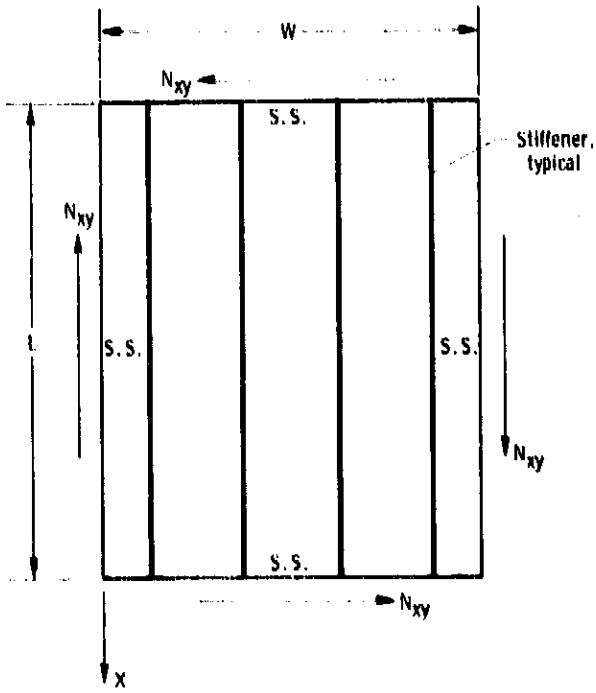

Figure 6.- Finite stiffened panel of length L and width W, simply supported on all four edges, and subject to shear load N_{xy}.

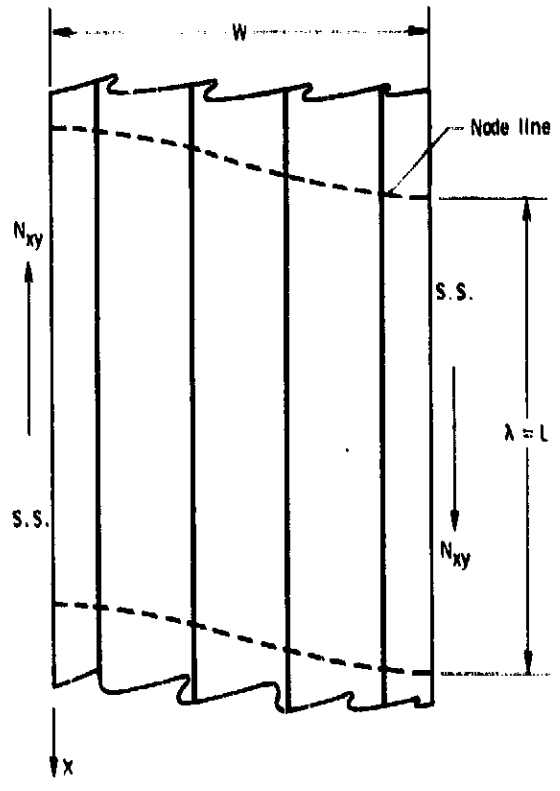

Figure 7.- Node lines given by VIPASA for shear buckling with $\lambda = L$.

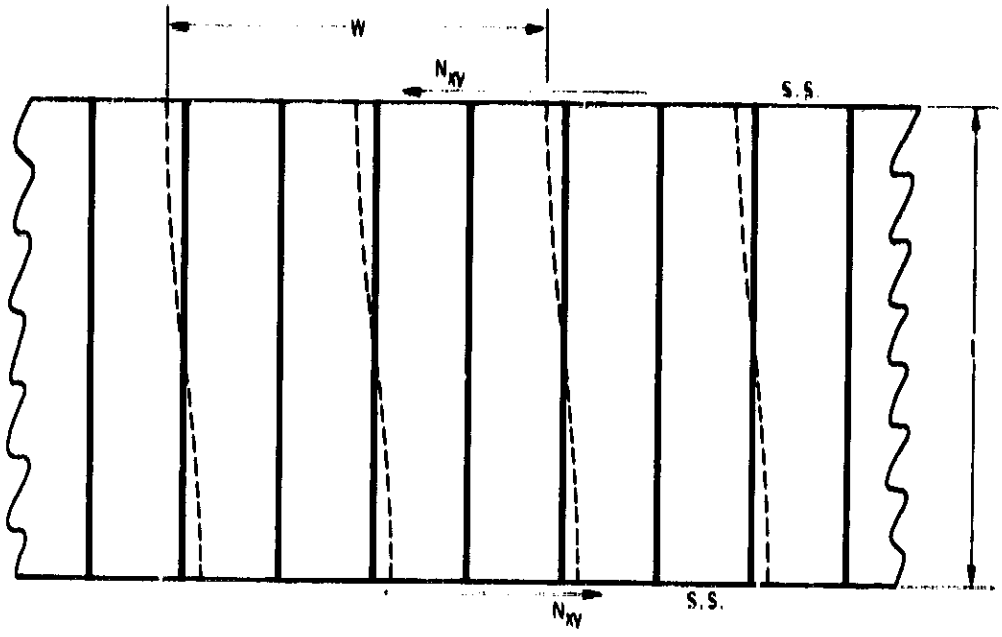

Figure 8.- Node lines for buckling of infinitely wide stiffened panel.

It is assumed that a better approximation to the solution for the finite panel would be obtained with the infinitely wide panel[1] shown in figure 8. Unfortunately, the mathematical model illustrated in figure 8 cannot be analyzed with VIPASA because VIPASA requires that the panel be uniform in the direction of the infinite dimension. However, the mathematical model obtained by smearing the stiffnesses of the stiffened panel of figure 8 can be analyzed with VIPASA. Using the definition of F given in equation (2), let $F_{s,90}$ be the value of F for the smeared orthotropic model rotated 90° as shown in figure 8.

In an attempt to adjust the smeared orthotropic solution $F_{s,90}$ to account for the effects of discrete stiffeners, the solution $F_{s,90}$ is multiplied by a correction factor $F_{d,0}/F_{s,0}$. Both $F_{d,0}$ and $F_{s,0}$ are calculatd with VIPASA using the infinitely long model of figure 7. The solution $F_{d,0}$ is obtained using discrete stiffeners - the usual VIPASA solution; $F_{s,0}$ is calculated with smeared

[1]That approach was used in reference 13. Stiffeners were treated as EI stiffeners.

stiffnesses. The correction factor is based on the assumption that the relationship between the smeared solution and the discrete solution for the infinitely long panel is approximately the same as that for the infinitely wide panel. If that assumption were correct, then $(F_{d,0}/F_{s,0})\ F_{s,90}$ would be the discrete solution for the infinitely wide panel of figure 8. In reference 11, that solution is denoted $F_{d,90}$.

$$F_{d,90} = \frac{F_{d,0}}{F_{s,0}}\ F_{s,90} \tag{3}$$

The mathematical models for the four solutions that appear in equation (3) are illustrated in figure 9.

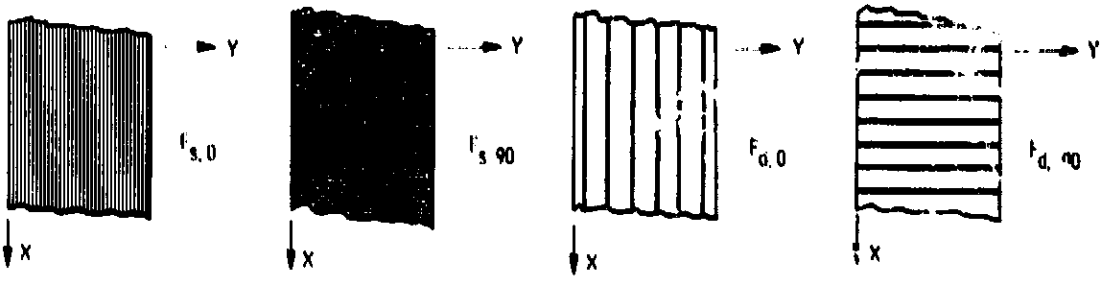

Figure 9.- Analysis models used to obtain adjusted solution for shear buckling.

Summary descriptions of the four solution are:

$F_{d,0}$ Standard VIPASA solution for $\lambda = L$.

$F_{s,0}$ Infinitely long orthotropic plate solution for the case $\lambda = L$ obtained with VIPASA by smearing the stiffnesses.

$F_{s,90}$ Infinitely wide orthotropic plate solution obtained with VIPASA by smearing the stiffnesses, rotating the direction of the stiffnesses by 90^{o}, and interchanging the N_x and N_y loads. The eigenvalue used is the lowest of the set for $\lambda = W, W/2, W/3, \ldots$ where W is the width of the panel being studied. (fig. 6)

$F_{d,90}$ Obtained from equation (3). Does not involve an analysis.

In PASCO, if an adjusted analysis is selected for the $\lambda = L$ mode, the solution used for that mode is the smaller of $F_{d,90}$ and $F_{s,90}$. (However, $F_{d,0}$ is used as the lower bound for the solution).

The input parameter SHEAR is used to indicate whether the adjusted analysis is to be used for the $\lambda = L$ buckling load. If SHEAR = 0, the standard VIPASA analysis is used. If SHEAR ≠ 0, the adjusted analysis is used and the value of the twisting stiffness used in calculating the smeared orthotropic plate buckling load is the product of SHEAR and the value of the twisting stiffness calculated by equations (43) and (44) in reference 11. A value of SHEAR less than 1 is generally appropriate for a panel composed of closed section stiffeners, such as a hat-stiffened panel.

To summarize the various possibilities for F:

- When the adjusted shear analysis is used (SHEAR ≠ 0 and $\lambda = L$), F is the smaller of $F_{d,90}$ and $F_{s,90}$.
- For all other cases (SHEAR = 0 or $\lambda \neq L$), F is the usual VIPASA solution ($F_{d,0}$ when $\lambda = L$).

The adjusted analysis is an engineering approximation, and engineering judgment should be used in its application. For example, the degree to which the smeared orthotropic solutions $F_{s,0}$ and $F_{s,90}$ are good approximations to the corresponding discrete stiffener solutions depends, in part, on the buckle mode shape of the smeared solution. In both cases, the buckle half-wavelength transverse to the stiffening should be at least 2.5 times the stiffener spacing. In subsequent sections of this report, calculations for several stiffened panels are presented to assess the validity of the adjusted analysis. Based on these calculations, recommendations for using the adjusted analysis are presented in the section entitled, DISCUSSION OF RESULTS. All of these recommendations involve a reduction in the buckling load predicted by the adjusted analysis.

STIFFENED PANEL EXAMPLES

Six stiffened panels were analyzed with PASCO and with the general finite element structural analysis codes EAL (refs. 6, 7) and STAGS (refs. 8, 9) to evaluate the shear buckling analyses (VIPASA and the adjusted analysis) in PASCO. Results of these analyses are presented in this section. Four of the six panels had blade stiffeners, one panel had hat stiffeners, and one panel was a corrugated panel. All panels were 76.2 cm (30 in.) square and had six equally-spaced stiffeners. The loadings were combinations of longitudinal compression (N_x) and shear (N_{xy}). STAGS results are presented only for the pure shear loadings and only for the first four examples--the blade stiffened panels. The VIPASA results provide an accurate check of the EAL model for pure longitudinal compression, and the STAGS results for the first four examples provide an independent check of the EAL results for pure shear. All standard VIPASA solutions (not the smeared orthotropic solutions) include the effect of anisotropic bending stiffness terms for each plate element making up the panel cross section.

A schematic drawing showing the loading and overall dimensions for the six example cases is shown in figure 10. The manner in which the applied loads were distributed over the cross section--the prebuckling stress state--is discussed in reference 11. In particular, the N_x load was distributed assuming uniform strain ϵ_x of the panel cross section with free transverse expansion of each plate element, so that N_{y_i} was zero. Buckling boundary conditions were simple support on all four edges. These boundary conditions are defined in figure 10. The panel cross sections were treated as collections of lines with no offsets to account for thicknesses. (Offsets are available in PASCO.) The first example is discussed in greater detail than the other examples.

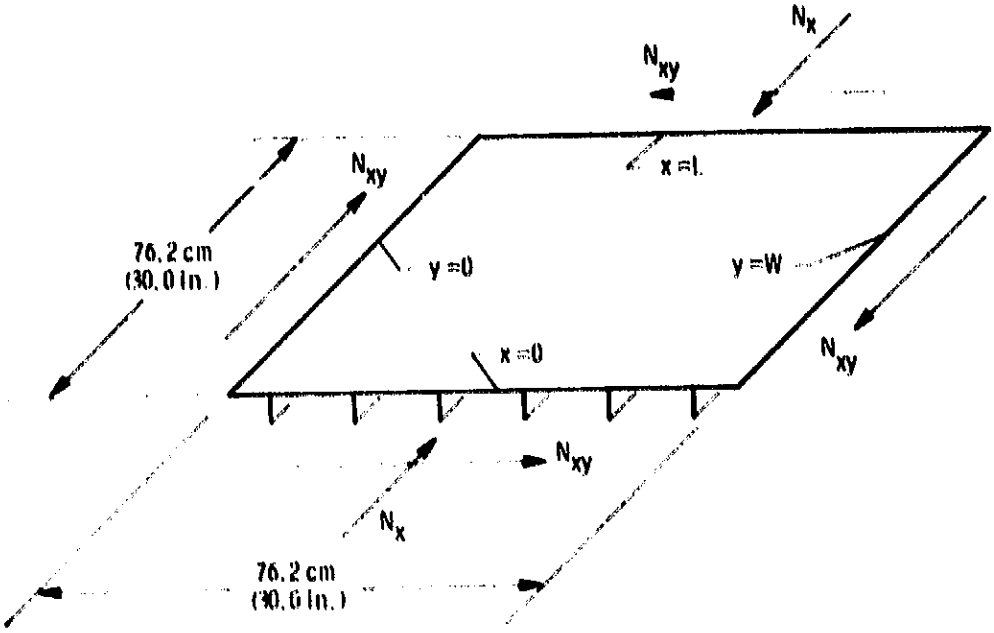

Buckling boundary conditions are simple support on all four edges

$x = 0, l$: u and $\frac{\partial w}{\partial x}$ are unrestrained, $v = w = 0$

$y = 0, W$: v and $\frac{\partial w}{\partial y}$ are unrestrained, $u = w = 0$

Figure 10.- Loading, dimensions, and boundary conditions for stiffened panel examples.

Example 1 - Composite Blade-Stiffened Panel

Panel description. - A repeating element of the composite blade-stiffened panel is shown in figure 11. Element widths are also shown. The wall construction for each plate element is given in table I. Only half the laminate is defined for each plate element because all laminates are symmetric. Plate element numbers are indicated by the circled numbers in figure 11. Fiber orientation angles are measured with respect to the X axis, which is parallel to the stiffener direction.

Values of Young's moduli, shear modulus, and Poisson's ratio for the graphite-epoxy material used in the calculations for this example are given in table II.

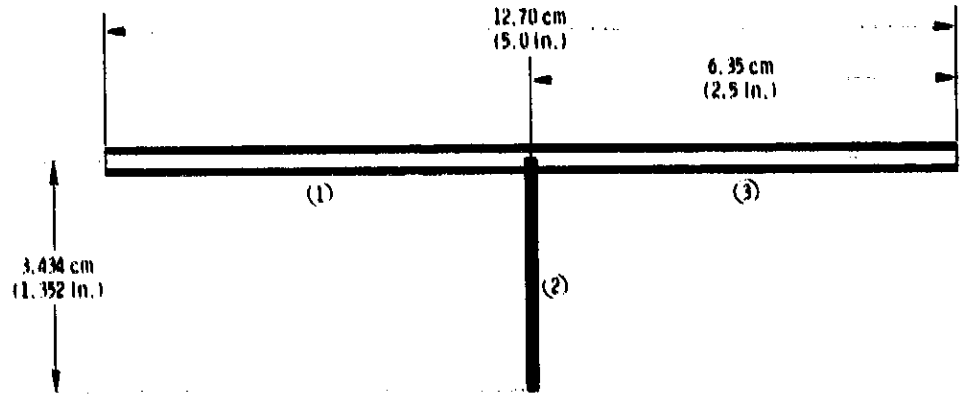

Figure 11.- Repeating element for example 1, composite blade-stiffened panel.

PASCO input. - Sample PASCO input for this example is shown in figure 12. In this input, the loading is $N_x = 1000$, $N_{xy} = 1000$ which means that a solution is sought for the case $N_x = N_{xy}$. ICARD input is included in order to get detailed plots of buckling mode shapes. The repeating element shown in figure 11 was generated with PASCO input.

```
***** EXAMPLE 1, COMPOSITE BLADE-STIFFENED PANEL *****
$CONDAT
$
$PANEL
B=2.5, 1.352, 2.5,
T=.0055, .0055, .0495, .0055, .011,
THET=45, 0, 90, 45, 0,
KWALL(1,1)=1,-1,-1,1,2,3,
KWALL(1,2)=4,-4,-4,4,5,
IWALL=1,2,1,
HCARD=4,-4,2,90,0,
      2,121,4,
      4,5,1,3,-121,
ICARD=5,1,3,1,-909,0900,
      3,2,3,4,
      3,3,4,3,
      3,4,-909,0900,
NOBAY=6,
ICREP=6,
EL=30,
MINLAM=30,
IBC=1,
SHEAR=1,
IP=2,
NX=1000.,
NXY=1000.,
$
$MATER
E1=19.E6,   E2=1.89E6,  E12=.93E6,  ANU1=.38,  RHO=.0571,
ALFA1(1)=-.005E-6,     ALFA2(1)=21.8E-6,
ALLOW(1,1)= 2, .004, -.004, .004, -.004, .01,
$
```

Figure 12.- Sample PASCO input for example 1, composite blade-stiffened panel.

EAL model. - The single finite element type used in the EAL model for this and the other examples is a four-node, quadrilateral, combined membrane and bending element. Both the membrane and bending stiffness matrices for the element are based on the assumed stress, hybrid formulation of Pian (refs. 6 and 14). The buckling or geometric stiffness matrix for the element is based on a conventional displacement formulation that includes terms allowing inplane (u and v displacements) as well as out-of-plane (w displacements) buckling modes. The Pian membrane formulation allows a single element across the depth of a blade stiffener to accurately represent its overall inplane bending behavior. The EAL designation for this element is E43.

The finite element grid chosen for the EAL model is shown in figure 13. Two elements are used along the depth of the blade, four elements are used between blades, and 36 elements are used along the length, making a total of 1296 elements and 1369 nodes. A more refined model consisting of three elements along the depth of the blade, four elements between blades, and 48 elements along the length was used as a check for selected loadings. (In all cases, the differences in the results for the two models were negligible).

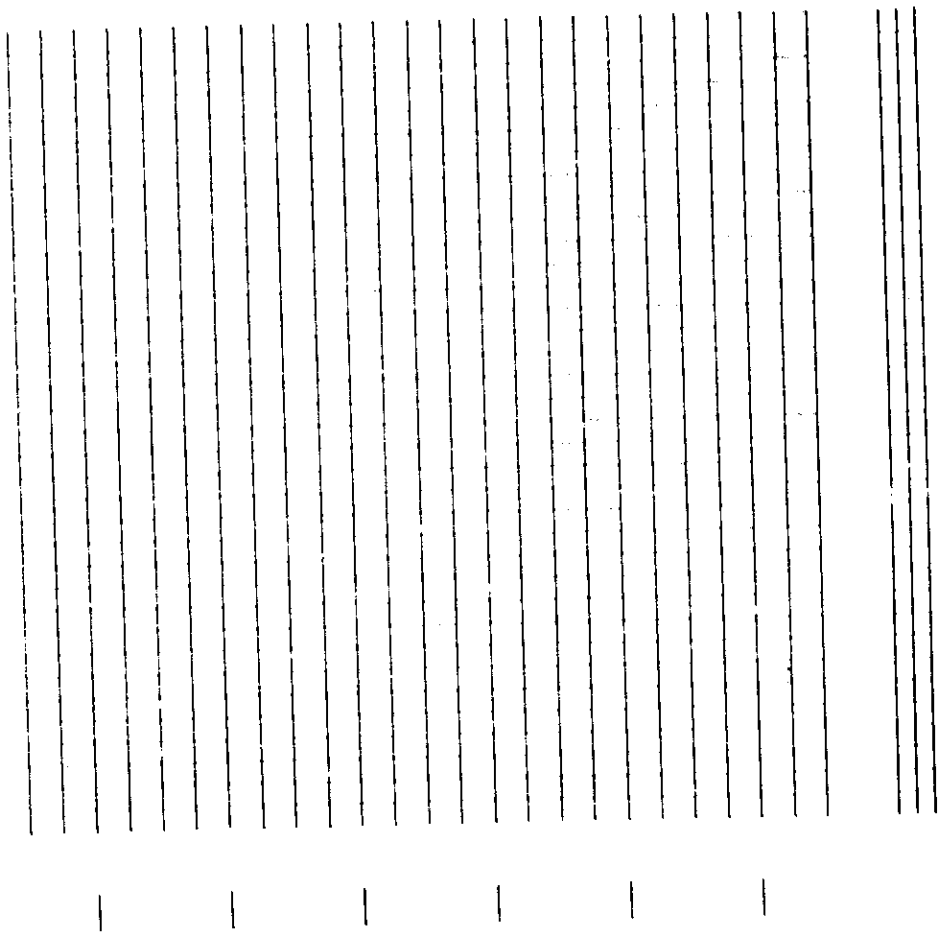

(a) Three views of model.

Figure 13.- EAL finite element model for example 1, composite blade-stiffened panel.

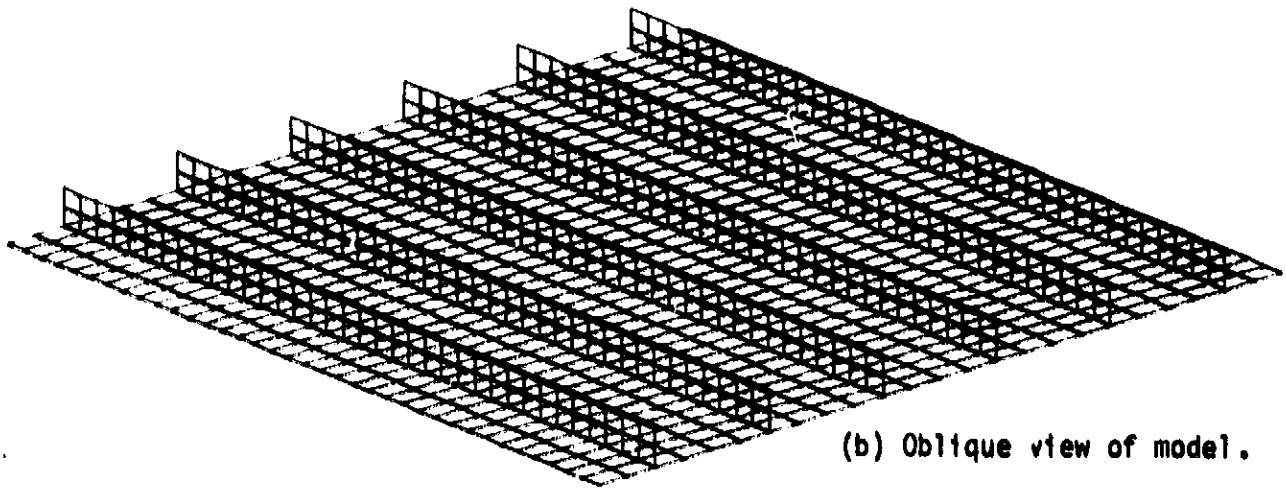

(b) Oblique view of model.

Figure 13.- Concluded.

It is recognized that the EAL model just described and the STAGS models described in the next section are more refined than models used in usual engineering calculations. However, since accuracy was an issue in this study and since relatively inexpensive and accurate procedures do not exist for calculating buckling loads when the loading involves shear, it was decided that benchmark calculations that differ from the exact solution by no more than approximately one percent were needed. Based on convergence studies and other comparisons, it is believed that the finite element calculations presented in this report meet this accuracy requirement.

STAGS model. - The single finite element type used in the STAGS model of this and the other examples is a six-node, triangular, combined membrane and bending element. The element is based on the Clough-Felippa triangle and has a displacement formulation. Midside nodes allow a single element across the depth of a blade stiffener to accurately represent its overall inplane bending behavior. The STAGS designation for this element is 422.

The finite element grid chosen for the STAGS model is shown in figure 14. The total number of triangular elements in the model is 2000. The total number of degrees of freedom in the model is 21541. A more refined model containing four elements between blades was used as a check for selected loadings.

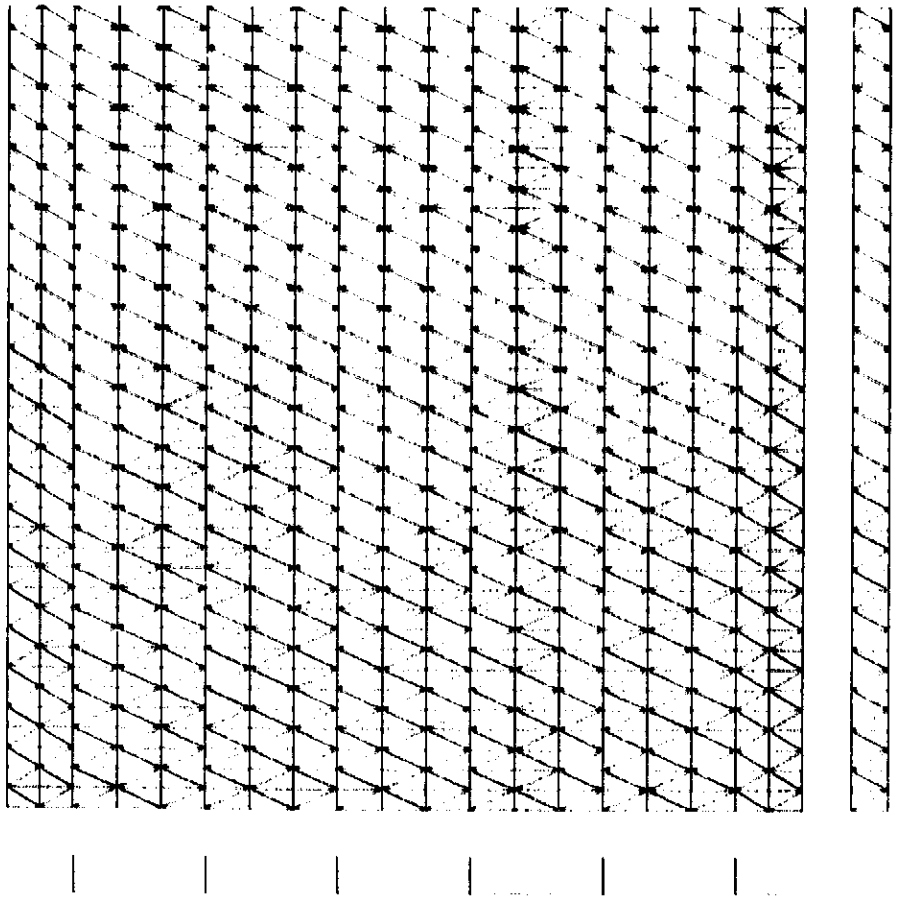

(a) Three views of model.

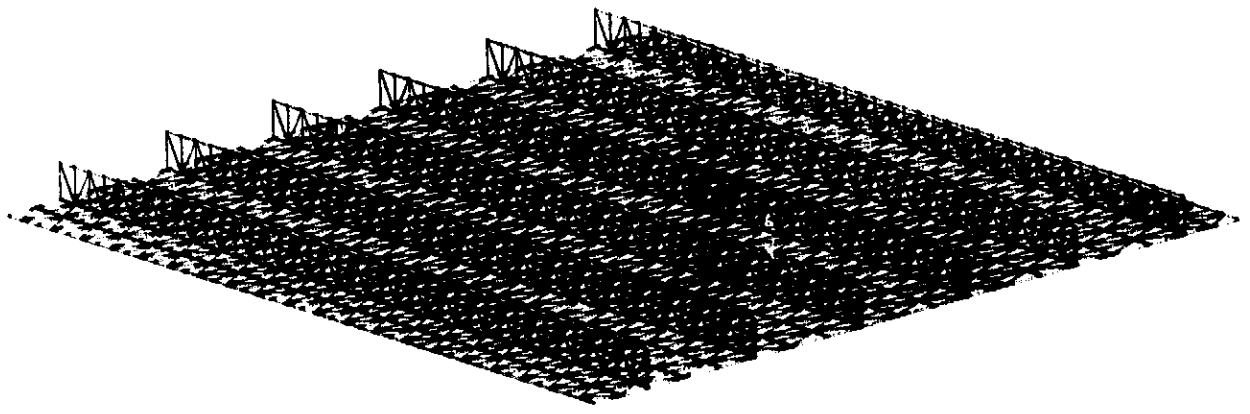

(b) Oblique view of model.

Figure 14.- STAGS finite element model for example 1, composite blade-stiffened panel.

Results. - Buckling results obtained with PASCO, EAL, and STAGS for this example are shown in figure 15. The curves indicate PASCO results, and the symbols indicate EAL and STAGS results. PASCO results are discussed first.

The dotted line at the top of the figure represents the standard VIPASA solution for half-wavelength λ equal to L/2 and is discussed subsequently. The four complete curves represent the four solution approaches that appear in figure 9 and are identified in the key for figure 15. The solid curve represents the standard VIPASA solution for λ = L and is denoted $F_{d,0}$. The curve $F_{s,0}$ below the solid curve and the curve $F_{s,90}$ above the solid curve represent orthotropic plate solutions obtained with VIPASA. These orthotropic plate solutions are explained in an earlier section entitled Adjusted Analysis for Shear. Each point of the curve $F_{s,0}$ represents a solution for λ = L where L is the panel length, and each point of the curve $F_{s,90}$ represents a solution for the lowest buckling load of the set λ = W, W/2, W/3,....where W is the panel width. The curve $F_{d,90}$ represents solutions obtained using equation (3).

The corners in the $F_{s,90}$ and $F_{d,90}$ curves that occur at N_x equal to approximately 130 kN/m (750 lb/in) indicate a change in mode shape for the $F_{s,90}$ solution. For N_x less than 130 kN/m, the buckling half-wavelength transverse to the stiffeners is equal to 38 cm (15 in.) which is three times the stiffener spacing. For N_x greater than 130 kN/m, the buckling half-wavelength transverse to the stiffeners is equal to 76 cm (30 in) which is six times the stiffener spacing. In both cases, the buckling mode shape meets the requirement that for $F_{s,90}$ to be valid, the buckle half-wavelength transverse to the stiffeners must be at least 2.5 times the stiffener spacing. Since the VIPASA solution is exact for loadings involving only N_x and N_y, both orthotropic solutions $F_{s,0}$ and $F_{s,90}$ give the same answer for N_{xy} = 0. For that reason, $F_{d,90}$ = $F_{d,0}$ for N_{xy} = 0.

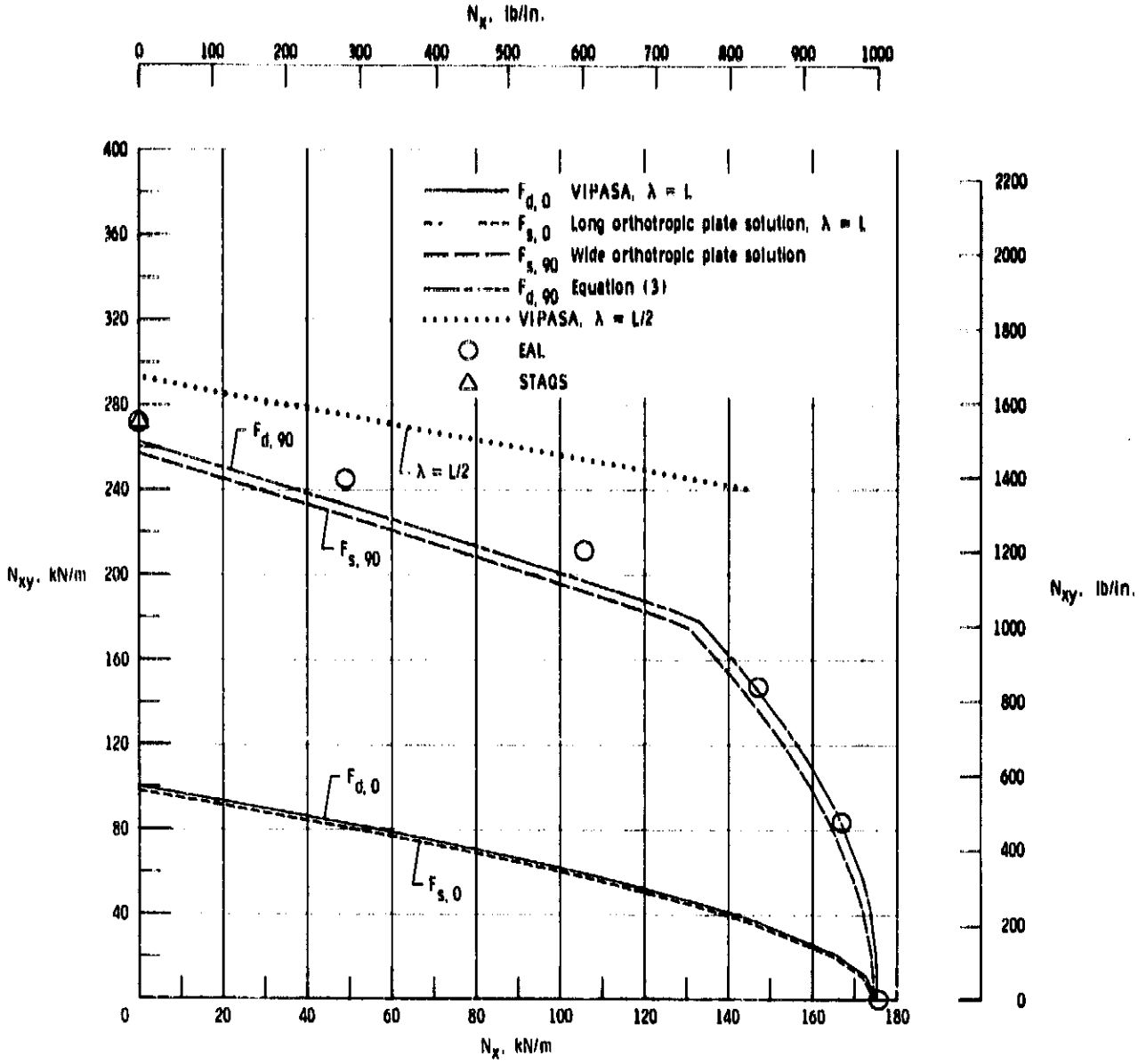

Figure 15.- Buckling load interaction obtained with PASCO, EAL, and STAGS for example 1, composite blade-stiffened panel.

As mentioned earlier, the dotted line at the top represents the standard VIPASA solution for λ = L/2. It is the λ = L/2 counterpart of the $F_{d,0}$ solution, which is for λ = L. Buckling modes with shorter wavelengths (λ = L/3, L/4,....) have even larger buckling loads.

For this example, short wavelength modes have higher buckling loads than the $F_{s,90}$ and $F_{d,90}$ solutions. Therefore, if an adjusted analysis is prescribed, the buckling interaction curve predicted by PASCO is the $F_{s,90}$

curve. (PASCO selects the lower of $F_{s,90}$ and $F_{d,90}$ for the $\lambda = L$ mode, as explained in a previous section.)

The circular symbols represent EAL results and the triangular symbol at $N_x = 0$ represents a calculation made with STAGS. The STAGS and EAL results at $N_x = 0$ agree to within 0.5 percent.

For this example, the infinitely wide orthotropic solution $F_{s,90}$ in PASCO and the adjusted analysis $F_{d,90}$ in PASCO give reasonably accurate estimates of the solution for all combinations of N_x and N_{xy}. For the loading $N_x = 0$, the solution $F_{s,90}$ (which, in this case, would be used by PASCO if an adjusted analysis were specified) is about five percent lower than the EAL and STAGS solutions. For this same loading, the standard VIPASA solution $F_{d,0}$ is about 63 percent lower than the EAL and STAGS solutions. For the loading $N_{xy} = 0$, the standard VIPASA solution and the EAL solution agree to within 0.3 percent.

Detailed comparisons and benchmark calculations for six loadings are presented in table III. In this table, the quantity denoted FACTOR is the solution in terms of a scale factor for the specified loading. For example, for the loading $N_x = 350.3$ kN/m, $N_{xy} = 175.1$ kN/m ($N_x = 2000$ lb/in, $N_{xy} = 1000$ lb/in) the EAL solution of FACTOR = 0.4764 means that the solution is $N_x = 0.4764 \times 350.3 = 166.9$ kN/m (952.8 lb/in), $N_{xy} = 0.4764 \times 175.1 = 83.42$ kN/m (476.4 lb/in).

Finally, the buckling mode shape obtained with EAL for the case $N_x = 0$ is shown in figure 16. The contour plot shown in figure 16(b) shows that the buckling half-wavelength transverse to stiffeners is approximately equal to three times the stiffener spacing, which was predicted by the $F_{s,90}$ solution. The buckling mode shapes obtained with PASCO and EAL for the case $N_{xy} = 0$ are shown in figure 17.

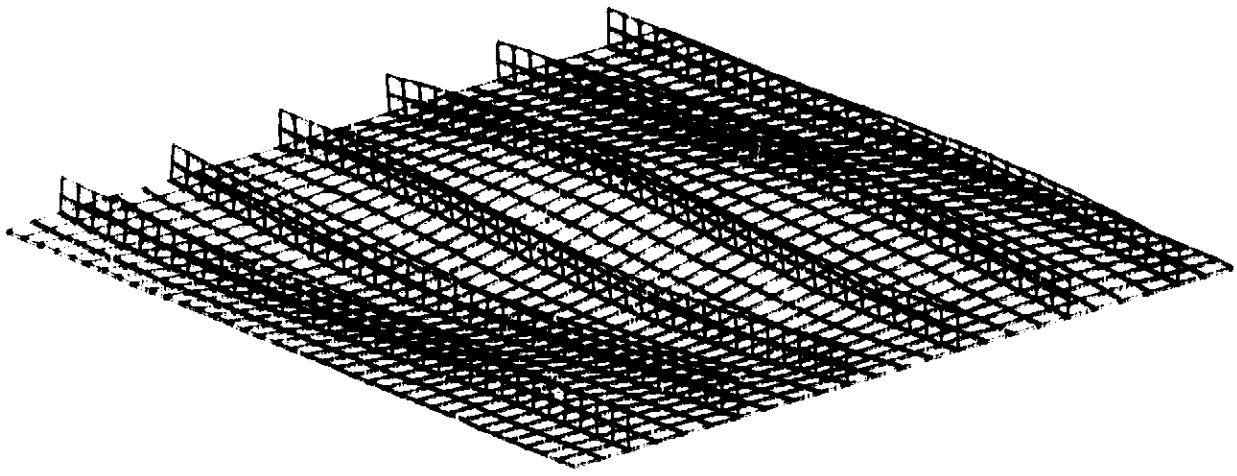

(a) Oblique view.

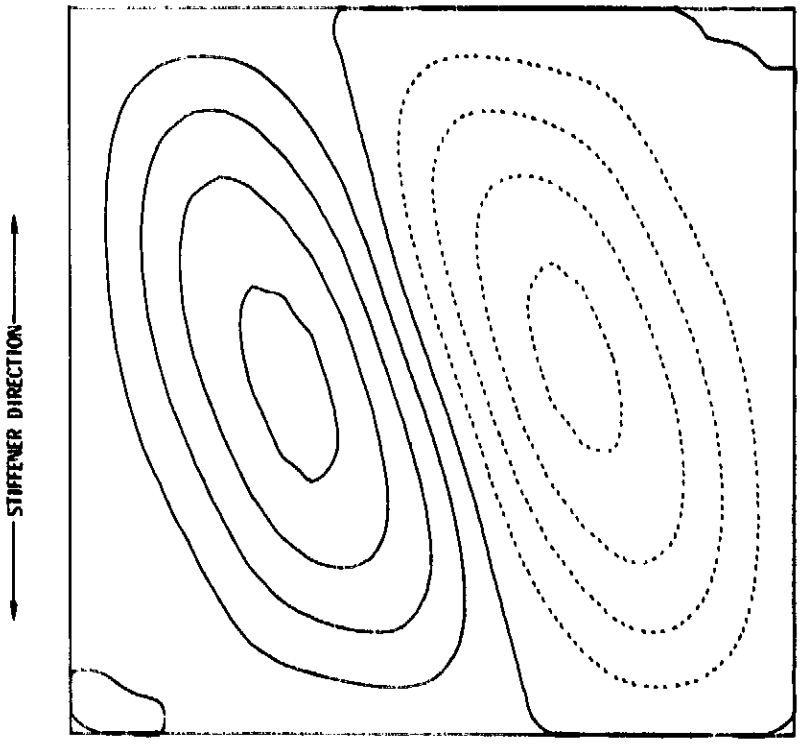

(b) Contour plot.

Figure 16.- Shear buckling mode shape obtained with EAL for example 1, composite blade-stiffened panel.

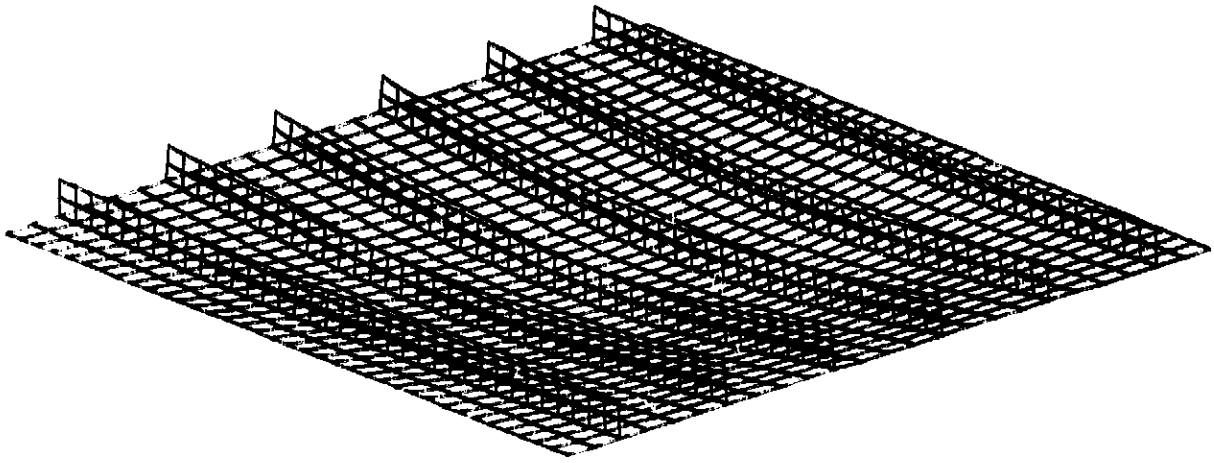

(a) Mode shape obtained with EAL.

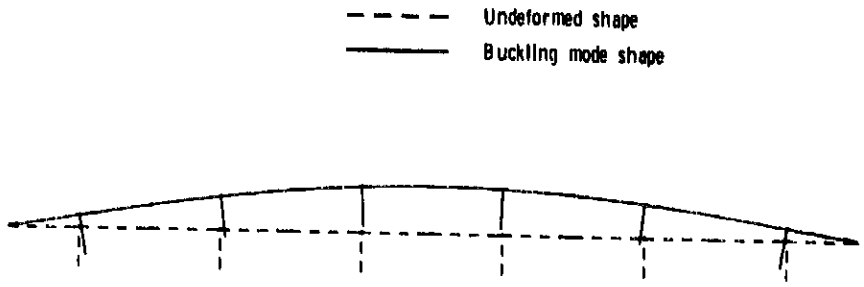

(b) Mode shape obtained with PASCO.

Figure 17.- Buckling mode shape for pure longitudinal compression for example 1, composite blade-stiffened panel.

TABLE I.- WALL CONSTRUCTION FOR EACH PLATE ELEMENT IN EXAMPLE 1, COMPOSITE BLADE-STIFFENED PANEL

Layer Number, Starting With Outside Layer	Thickness		Fiber Orientation, Deg
	cm	in	
Plate Elements 1 and 3			
1	.01397	.00550	45
2	.01397	.00550	-45
3	.01397	.00550	-45
4	.01397	.00550	45
5	.01397	.00550	0
6	.12573	.04950	90
Plate Element 2			
1	.01397	.00550	45
2	.01397	.00550	-45
3	.01397	.00550	-45
4	.01397	.00550	45
5	.02794	.01100	0

TABLE II.- LAMINA PROPERTIES OF GRAPHITE-EPOXY MATERIAL USED IN CALCULATIONS

Symbol	Value in SI Units	Value in U.S. Customary Units
E_1	131. GPa	19×10^6 psi
E_2	13.0 GPa	1.89×10^6 psi
E_{12}	6.41 GPa	$.93 \times 10^6$ psi
μ_1	.38	.38

TABLE III.- BUCKLING LOADS FOR EXAMPLE 1, COMPOSITE BLADE-STIFFENED PANEL

Loading				FACTOR						
N_x		N_{xy}								
$\frac{kN}{m}$	$\frac{lbf}{in}$	$\frac{kN}{m}$	$\frac{lbf}{in}$	$F_{d,0}$	$F_{s,0}$	$F_{s,90}$	$F_{d,90}$	$\lambda = L/2$	EAL	STAGS
0	0	175.1	1000	.5721	.5598	1.4683	1.5005	1.6641	1.5525	1.5565
35.0	200	175.1	1000	.5353	.5241	1.3098	1.3378	1.5614	1.3985	
87.6	500	175.1	1000	.4862	.4764	1.1222	1.1452	1.4248	1.2060	
175.1	1000	175.1	1000	.4182	.4104	.8222	.8379	1.2357	.8397	
350.3	2000	175.1	1000	.3200	.3150	.4690	.4765		.4764	
175.1	1000	0	0	1.0005	.9970	.9970	1.0005		1.0030	

Example 2 - Metal Blade-Stiffened Panel

Panel description. - A repeating element of the metal blade-stiffened panel is shown in figure 18. Element widths and thicknesses are also shown. The material properties used in the calculations are E = 72.4 GPa (10.5×10^6 psi), μ = .32.

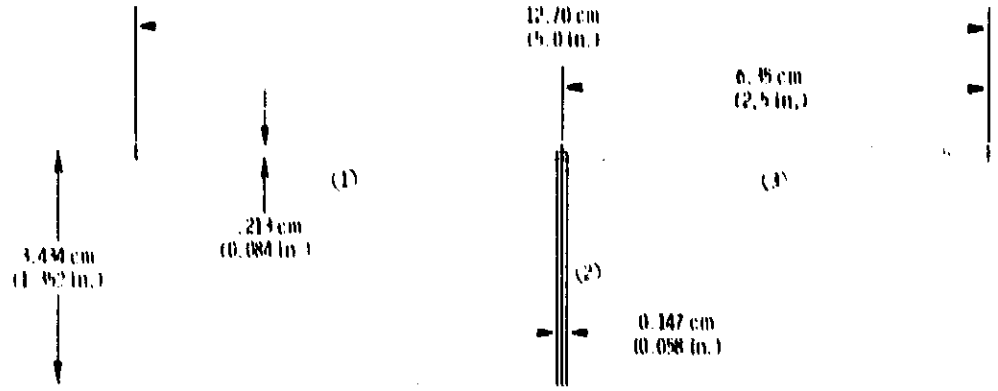

Figure 18.- Repeating element for example 2, metal blade-stiffened panel.

PASCO input. - Sample PASCO input for this example is shown in figure 19. As is the case with all examples in this report, ICARD input is included to get detailed plots of buckling mode shapes. The same numerical results are obtained when the modeling is carried out with HCARD input only. The repeating element shown in figure 18 was generated with PASCO input.

EAL and STAGS models. - The same finite element and grid pattern used in the EAL model of the first example are used in this example. The finite element and grid pattern used in the STAGS model of the first example are also used in this example.

Results. - The same general approach used for presenting the buckling results in the first example is used in this and subsequent examples. Buckling results obtained with PASCO, EAL, and STAGS for this example are shown in

```
*****  EXAMPLE 2, METAL BLADE-STIFFENED PANEL  *****
$CONDAT
$
$PANEL
R=2.5, 1.352, 2.5,
T=.042, .029,
THET= 0, 0,
KWALL(1,1)=1,
KWALL(1,2)=2,
TWALL=1,2,1,
HCARD=4,-4,2,90,0,
      2,121,4,
      4,5,1,3,-121,
ICARD=5,1,3,1,-909,0900,
      3,2.3,4,
      3,3,4,3,
      3,4,-909,0900,
ICREP=6,
NOBAY=6,
SHEAR=1,
EL=30,
MINLAM=30,
IBC=1,
IP=2,
NX=1000.,
NLAM=1,2,3,
$
$MATER
E1=10.5E6, E2=10.5E6, E12=3.9772727E6, ANU1=.32, RHO=.1,
ALFA1(1)=-.005E-6,      ALFA2(1)=21.8E-6,
ALLOW(1,1)= 2, .004, -.004, .004, -.004, .01,
$
```

Figure 19.- Sample PASCO input for example 2, metal blade-stiffened panel.

figure 20. Curves indicate PASCO results, and symbols indicate EAL and STAGS results. PASCO results are described first.

A portion of the standard VIPASA solution for $\lambda = L/2$, shown by the dotted line near the top of the figure, is below the $F_{s,90}$ and $F_{d,90}$ solutions. Therefore, if the adjusted analysis approach is selected, this portion of the dotted line is an upper bound for the PASCO load interaction curve.

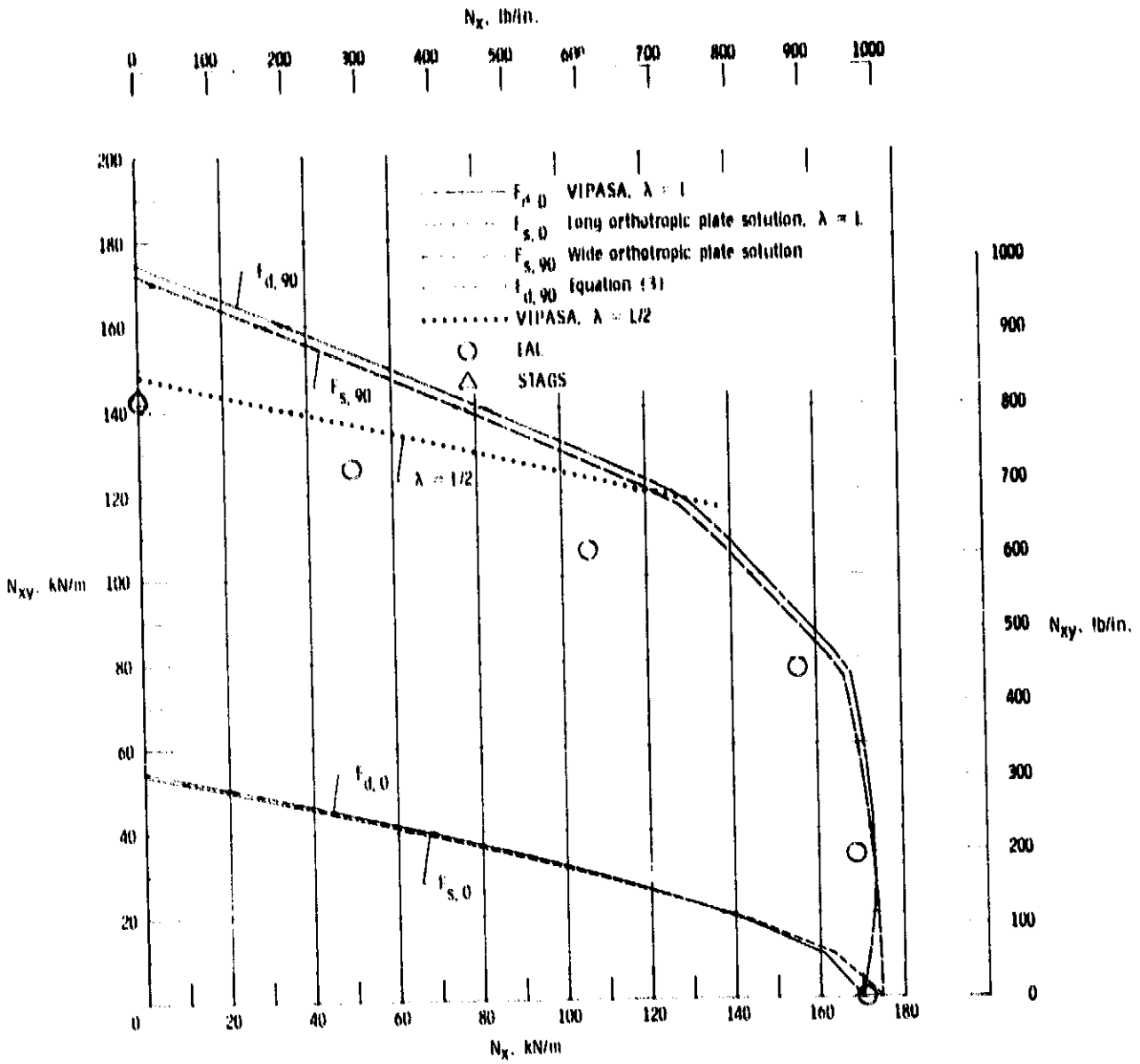

Figure 20.- Buckling mode interaction obtained with PASCO, EAL, and STAGS for example 2, metal blade-stiffened panel.

The corners in the $F_{s,90}$ and $F_{d,90}$ curves that occur at N_x equal to approximately 130 kN/m (750 lb/in) and 170 kN/m (950 lb/in) indicate a change in mode shape for the $F_{s,90}$ solution. For values of N_x less than about 130 kN/m the buckling half-wavelength transverse to the stiffeners is equal to 25.4 cm (10 in.) which is twice the stiffener spacing. In this case, the buckling mode shape does not meet the requirement that for $F_{s,90}$ to be valid, the buckling half-wavelength transverse to the stiffeners must be at least 2.5 times the

stiffener spacing. For values of N_x greater than 130 kN/m but less than 170 kN/m, the buckling half-wavelength transverse to the stiffeners is 38 cm (15 in.) which is three times the stiffener spacing. For values of N_x greater than 170 kN/m, the buckling half-wavelength transverse to the stiffeners is 76 cm (30 in.) which is six times the stiffener spacing.

The EAL and STAGS results fall below both the $\lambda = L/2$ line and the $F_{s,90}$ curve, which indicates that for this case the adjusted analysis approach in PASCO is unconservative. For the $N_x = 0$ case, an examination of the EAL buckling mode shape (fig. 21) shows that the buckling mode is an overall mode ($\lambda = L$) rather than a $\lambda = L/2$ mode which might have been assumed because the $\lambda = L/2$ solution is near the EAL and STAGS solutions. One possible factor contributing to the error in the smeared orthotropic solution $F_{s,90}$ near $N_x = 0$ is, as pointed out in the previous paragraph, that the buckle

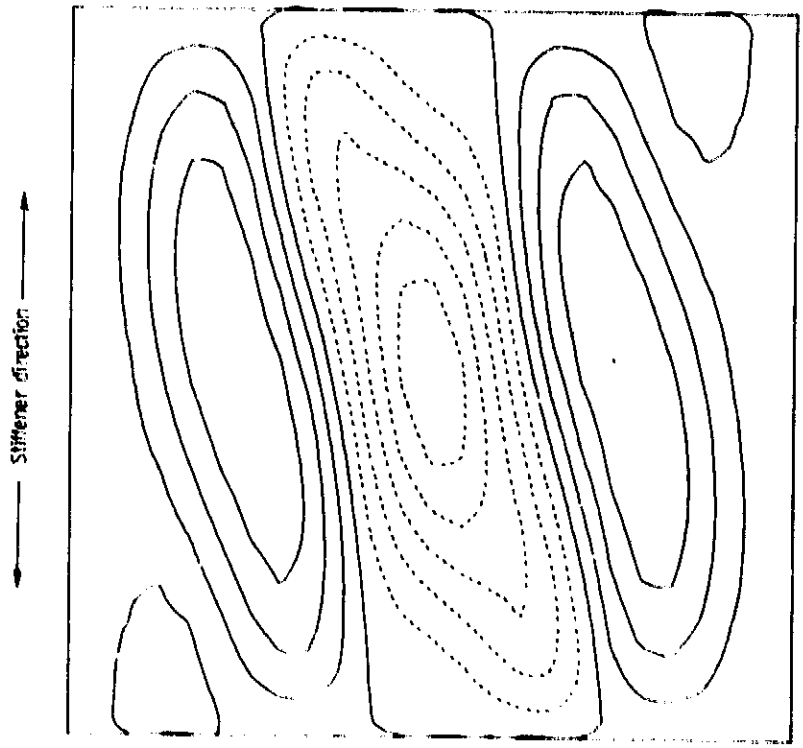

Figure 21.- Shear buckling mode shape obtained with EAL for example 2, metal blade-stiffened panel.

half-wavelength transverse to the stiffeners is too short to be a valid solution. These results and results for subsequent examples show the danger of depending upon a smeared orthotropic solution--even if the conservative assumption is made that the panel is infinitely wide rather than finite.

Detailed comparisons of solutions from PASCO, EAL, and STAGS for six loadings are presented in table IV. The buckle mode shape obtained with PASCO for the case $N_{xy} = 0$ is shown in figure 22.

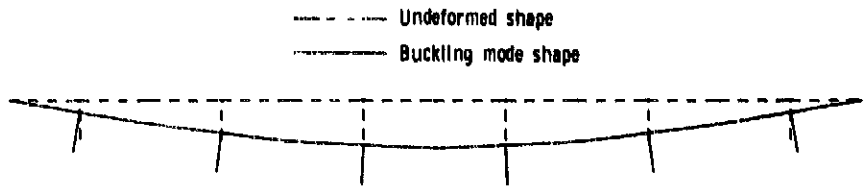

Figure 22.- Buckling mode shape for pure longitudinal compression, obtained with PASCO for example 2, metal blade-stiffened panel.

TABLE IV.- BUCKLING LOADS FOR EXAMPLE 2, METAL BLADE-STIFFENED PANEL

Loading				FACTOR						
N_x		N_{xy}								
$\frac{kN}{m}$	$\frac{lbf}{in}$	$\frac{kN}{m}$	$\frac{lbf}{in}$	$F_{d,0}$	$F_{s,0}$	$F_{s,90}$	$F_{d,90}$	$\lambda = L/2$	EAL	STAGS
0	0	175.1	1000	0.3118	0.3073	0.9823	0.9967	0.8450	0.8138	.8179
70.0	400	175.1	1000	.2877	.2838	.8423	.8539	.7742	.7195	
175.1	1000	175.1	1000	.2568	.2536	.6879	.6964	.6849	.6061	
350.3	2000	175.1	1000	.2159	.2137	.4637	.4683		.4444	
875.6	5000	175.1	1000	.1413	.1409	.1975	.1980		.1929	
175.1	1000	0	0	.97103	.99695	.97695	.97103		.9759	

Example 3 - Heavily-Loaded Composite Blade-Stiffened Panel

Panel description. - A repeating element of the heavily-loaded composite blade-stiffened panel is shown in figure 23. The wall construction for each plate element is given in table V. Only half the laminate is defined for each plate element because all laminates are symmetric. Plate element numbers are indicated by the circled numbers in figure 23. Values for material properties are the same as those used in example 1 and are given in table II.

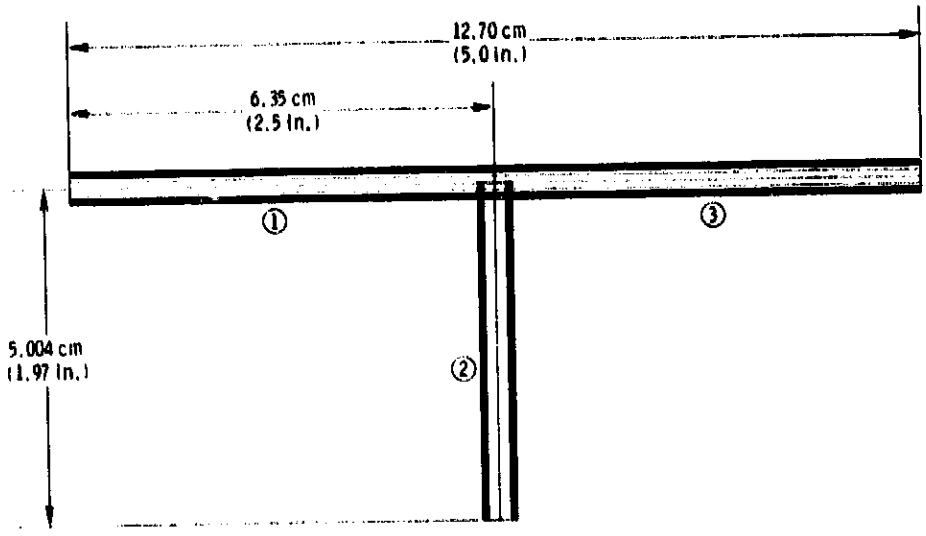

Figure 23.- Repeating element for example 3, heavily-loaded composite blade-stiffened panel.

PASCO input and EAL and STAGS models. - Sample PASCO input for this example is shown in figure 24. The same finite elements and grid patterns used in the EAL and STAGS models of the first example are used in this example.

Results. - Buckling results obtained with PASCO, EAL, and STAGS are shown in figure 25. The four complete curves represent the four PASCO solutions for overall buckling. The dotted lines indicate standard VIPASA solutions for λ = L/2, L/4, and L/5. If the adjusted analysis approach is selected, these

```
***** EXAMPLE 3, COMPOSITE BLADE-STIFFENED PANEL, HEAVILY LOADED *****
 $CONDAT
 $
 $PANEL
 GRANGE=10,
 B=2.5, 1.97, 2.5,
 T=.00637, .0249, .0416, .00823, .0675,
 THET=45, 0, 90, 45, 0,
 KWALL(1,1)=1,-1,-1,1,2,3,
 KWALL(1,2)=4,-4,-4,4,5,
 IWALL=1,2,1,
 HCARD=4,-4,2,90,0,
       2,121,4,
       4,5,1,3,-121,
 ICARD=5,1,3,1,-909,0900,
       3,2,3,4,
       3,3,4,3,
       3,4,-909,0900,
 NOBAY=6,
 ICREP=6,
 EL=30,
 MINLAM=30,
 IBC=1,
 NLAM=1,2,3,
 IP=2,
 NX=1000.,
 $
 $MATER
 E1=19.E6,   E2=1.89E6,  E12=.93E6,  ANU1=.38,  RHO=.0571,
 ALFA1(1)=-.005E-6,     ALFA2(1)=21.8E-6,
 ALLOW(1,1)= 2, .004, -.004, .004, -.004, .01,
 $
```

Figure 24.- Sample PASCO input for example 3, heavily-loaded composite blade-stiffened panel.

dotted lines form an upper bound for the PASCO load interaction curve.

For values of N_x less than about 1600 kN/m (9000 lb/in) the buckling mode shape for the $F_{s,90}$ solution does not meet the requirement that for $F_{s,90}$ to be valid, the buckling half-wavelength transverse to the stiffeners must be at least 2.5 times the stiffener spacing. For N_x less than 700 kN/m (4000 lb/in) the buckling half-wavelength transverse to the stiffeners is 1.5 times the stiffener spacing. For N_x greater than about 700 kN/m (4000 lb/in) but less than about 1600 kN/m (9000 lb/in) the buckling half-wavelength trans-

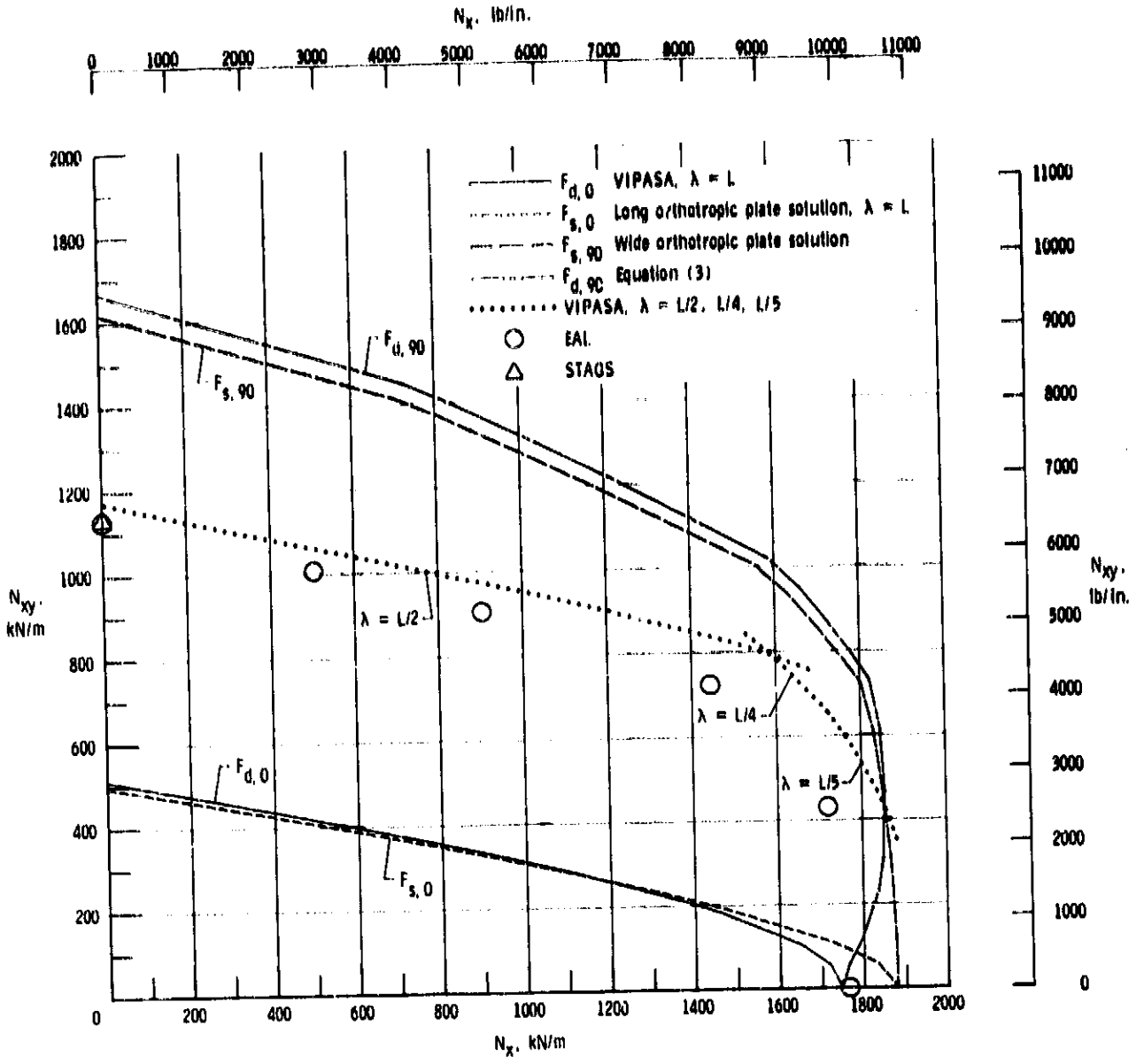

Figure 25.- Buckling load interaction obtained with PASCO, EAL, and STAGS for example 3, heavily-loaded composite blade-stiffened panel.

verse to the stiffeners is 2.0 times the stiffener spacing. For N_x greater than about 1600 kN/m but less than about 1800 kN/m, the buckling half-wavelength transverse to the stiffeners is 3.0 times the stiffener spacing.

For the loading $N_{xy} = 0$, the smeared orthotropic solutions $F_{s,0}$ and $F_{s,90}$ overestimate the buckling load by about 7.6 percent. For that reason, there is a bulge to the right in the load interaction curve that would be used by

PASCO if the adjusted analysis approach is selected. This bulge to the right represents incorrect solutions; predicted critical values of N_x that are greater than the value for $N_{xy} = 0$ should be disregarded. This bulging phenomenon also exists in other examples in this report.

The EAL and STAGS results fall below the $\lambda = L/2$, $L/4$, and $L/5$ curves which indicates that, for this case, the adjusted analysis approach in PASCO is unconservative. PASCO errors in the right-hand portion of the interaction curve would be reduced substantially if the bulge discussed in the previous paragraph were disregarded. As in example 2, the buckling mode for the EAL analysis at $N_x = 0$ is an overall mode--not a $\lambda = L/2$ mode.

Detailed comparisons of solutions from PASCO, EAL, and STAGS for six loadings are presented in table VI. The buckle mode shape obtained with EAL for the case $N_x = 0$ is shown in figure 26. The buckle mode shape obtained with PASCO for the case $N_{xy} = 0$ is shown in figure 27.

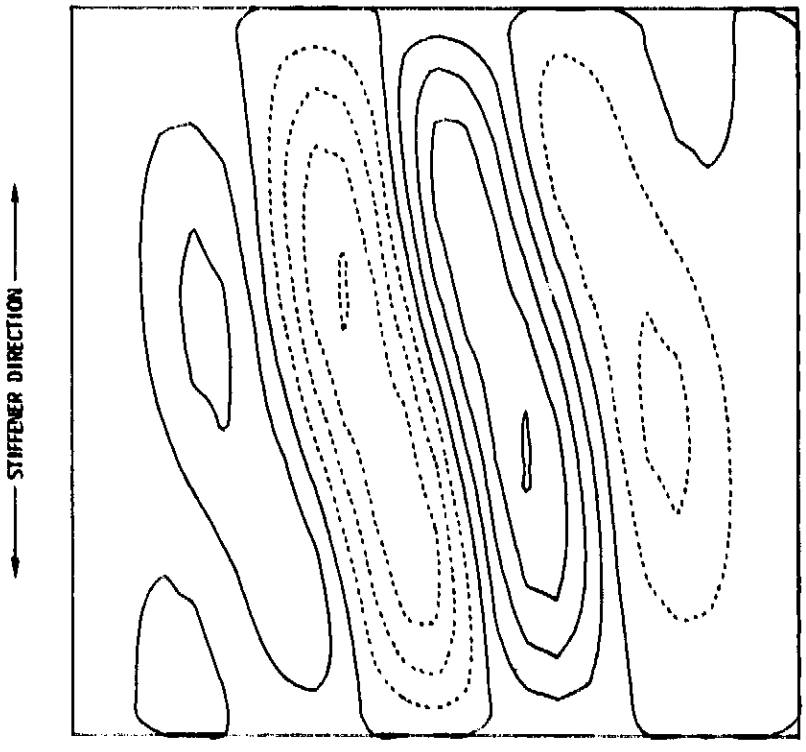

Figure 26.- Contour plot of shear buckling mode obtained with EAL for example 3, heavily-loaded composite blade-stiffened panel.

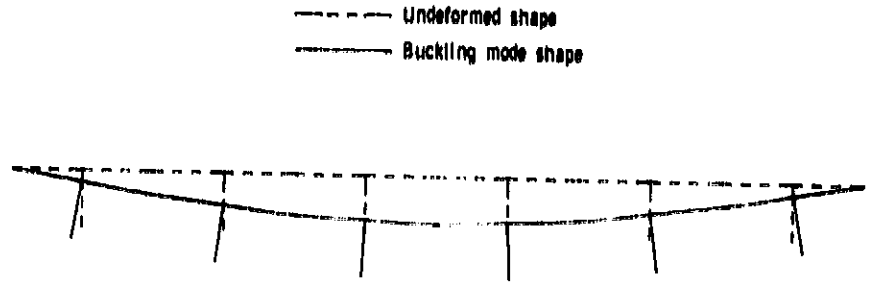

Figure 27.- Buckling mode shape for pure longitudinal compression, obtained with PASCO for example 3, heavily-loaded composite blade-stiffened panel.

TABLE V.- WALL CONSTRUCTION FOR EACH PLATE ELEMENT IN EXAMPLE 3, HEAVILY-LOADED COMPOSITE BLADE-STIFFENED PANEL

Layer Number, Starting With Outside Layer	Thickness		Fiber Orientation, Deg
	cm	in	
Plate Elements 1 and 3			
1	0.01618	0.00637	45
2	.01618	.00637	-45
3	.01618	.00637	-45
4	.01618	.00637	45
5	.06325	.02490	0
6	.10566	.04160	90
Plate Element 2			
1	0.02090	0.00823	45
2	.02090	.00823	-45
3	.02090	.00823	-45
4	.02090	.00823	45
5	.17145	.06750	0

TABLE VI.- BUCKLING LOADS FOR EXAMPLE 3, HEAVILY-LOADED COMPOSITE BLADE-STIFFENED PANEL

Loading				FACTOR						
N_x		N_{xy}								
$\frac{kN}{m}$	$\frac{lbf}{in}$	$\frac{kN}{m}$	$\frac{lbf}{in}$	$F_{d,0}$	$F_{s,0}$	$F_{s,90}$	$F_{d,90}$	$\lambda = L/2$	EAL	STAGS
0	0	175.1	1000	2.9225	2.8355	9.2435	9.5269	6.6998	6.4424	6.470
87.6	500	175.1	1000	2.6742	2.6052	8.0628	8.2764	6.0385	5.753	
175.1	1000	175.1	1000	2.4574	2.4031	6.7945	6.9480	5.4654	5.1630	
350.3	2000	175.1	1000	2.0997	2.0679	4.8627	4.9376	4.5367	4.124	
700.5	4000	175.1	1000	1.5964	1.5923	2.6424	2.6493		2.4543	
175.1	1000	0	0	9.9724	10.7300	10.7300	9.9724		10.076	

Example 4 - Metal Blade-Stiffened Panel With Thin Skin

Panel description. - A repeating element of the metal blade-stiffened panel with thin skin is shown in figure 28. Element widths and thicknesses are also shown. The material properties used in the calculations are E = 72.4 GPa (10.5×10^6 psi), μ = .32. Except for the thickness of the skin, this panel is the same as that used in Example 2.

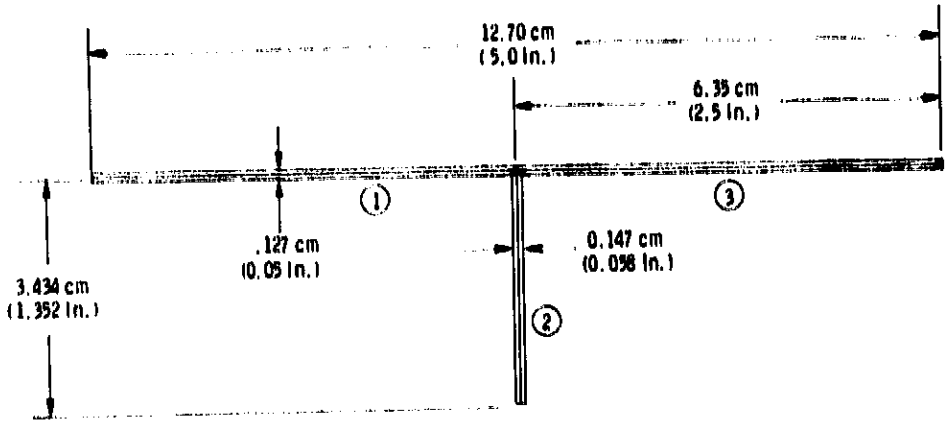

Figure 28.- Repeating element for example 4, metal blade-stiffened panel with thin skin.

PASCO input and EAL and STAGS models. - PASCO input for this example is the same as that given in figure 19 except that T(1) = .025. The same finite elements and grid patterns used in the EAL and STAGS models of the first example are used in this example.

Results. - Buckling results obtained with PASCO, EAL, and STAGS are shown in figure 29. The same general approach used for presenting buckling data in previous examples is used in this example.

The dotted curve represents the standard VIPASA solutions for λ = L/5 and L/6. If the adjusted analysis approach is selected, this dotted curve forms the PASCO load interaction curve. If the adjusted analysis approach is not selected, this dotted curve forms the right-hand portion of the PASCO load interaction curve.

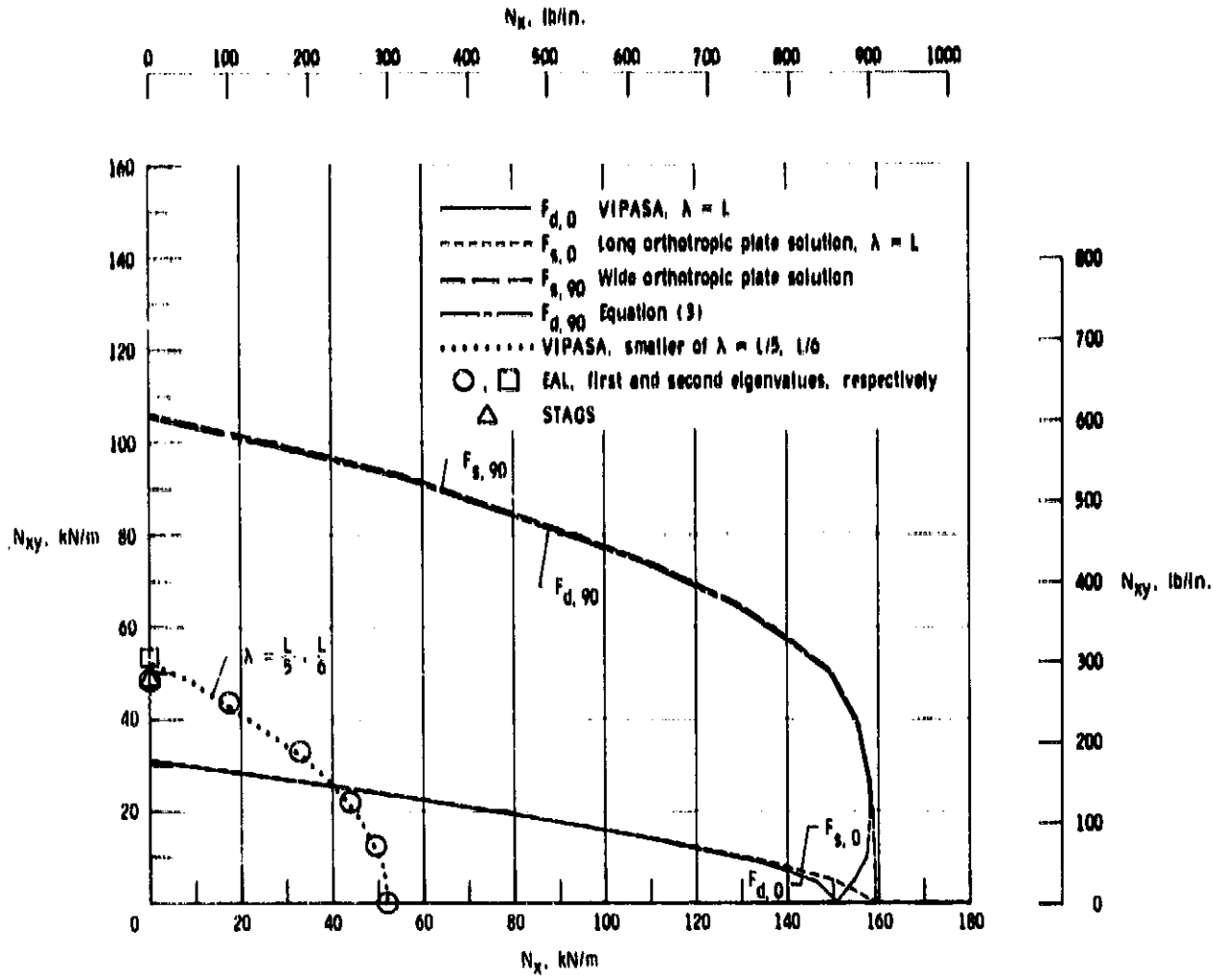

Figure 29.- Buckling load interaction obtained with PASCO, EAL, and STAGS for example 4, metal blade-stiffened panel with thin skin.

For values of N_x less than about 150 kN/m (850 lb/in), the buckling mode shape for the $F_{s,90}$ solution does not meet the requirement that for $F_{s,90}$ to be valid, the buckling half-wavelength transverse to the stiffeners must be at least 2.5 times the stiffener spacing. For example, at $N_x = 0$ the buckling half-wavelength transverse to the stiffeners is 1.2 times the stiffener spacing.

The EAL results are very near the PASCO short-wavelength results indicated by the dotted curve. Except for the case $N_x = 0$, the EAL results are slightly higher than the PASCO short-wavelength results. For the case $N_x = 0$, the lowest eigenvalue for both EAL and STAGS appears to be primarily an overall mode

rather than a local mode. The second eigenvalue from EAL, indicated by the square symbol, is a local mode. It is clear from this example that when the mode shape for the smeared orthotropic solution $F_{s,90}$ is in gross violation of the mode shape requirements (see previous paragraph), the adjusted analysis approach for predicting the overall buckling mode should be used with caution.

Detailed comparisons of solutions from PASCO, EAL and STAGS for six loadings are presented in table VII.

The buckle mode shape obtained with EAL for the case $N_x = 0$ is shown in figure 30. The buckle mode shapes obtained with EAL and PASCO for the case $N_{xy} = 0$ are shown in figure 31.

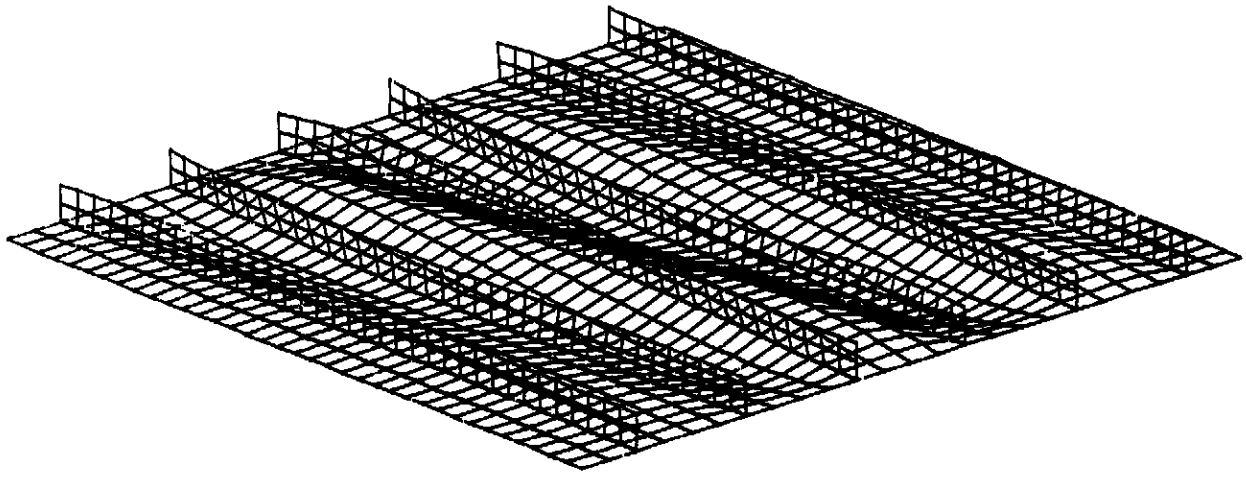

(a) Oblique view.

Figure 30.- Shear buckling mode shape obtained with EAL for example 4, metal blade-stiffened panel with thin skin.

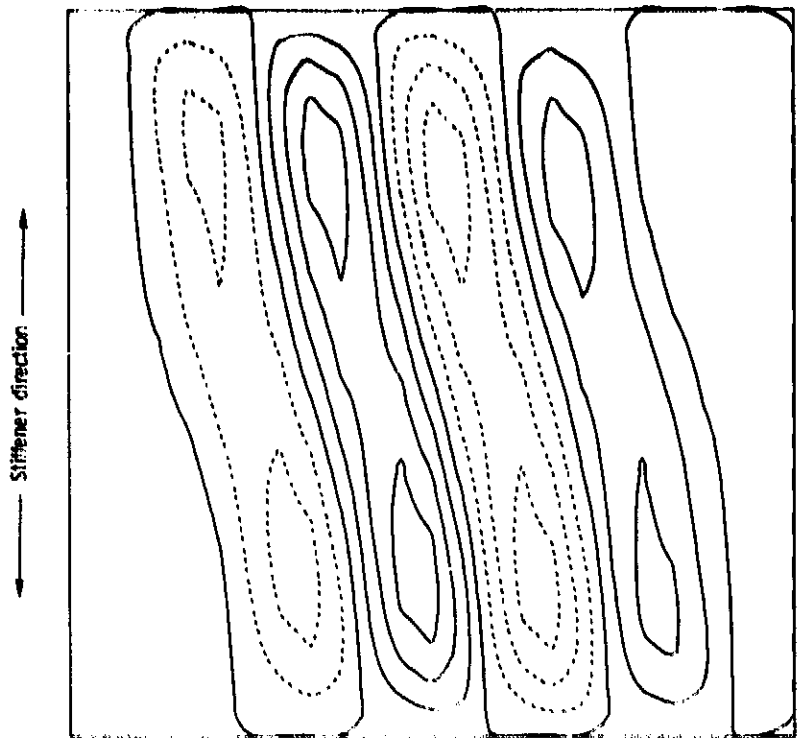

(b) Contour plot.

Figure 30.- Concluded.

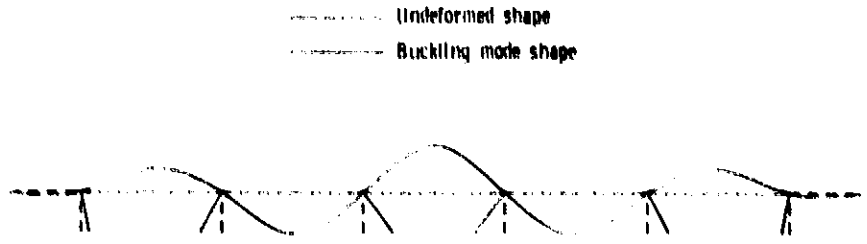

(a) Mode shape obtained with PASCO.

Figure 31.- Buckling mode shape for pure longitudinal compression for example 4, metal blade-stiffened panel with thin skin.

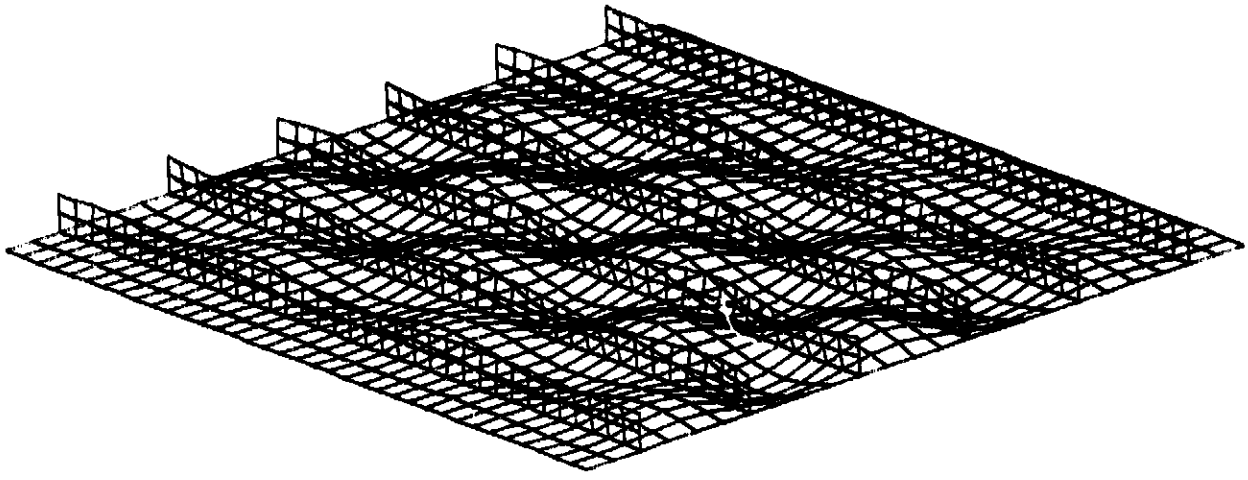

(b) Oblique view of mode shape obtained with EAL.

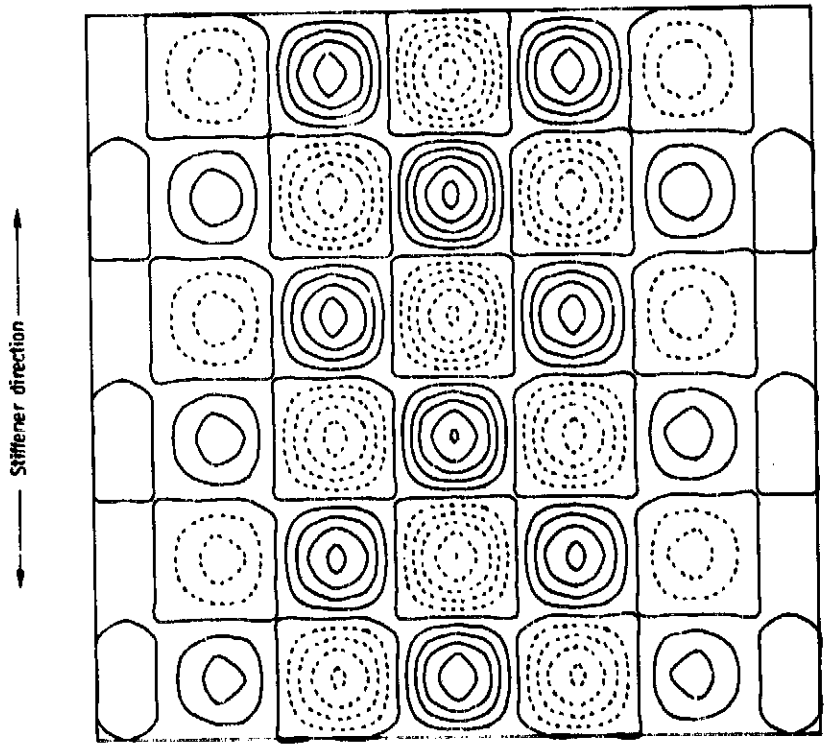

(c) Contour plot of mode shape obtained with EAL.

Figure 31.- Concluded.

TABLE VII.- BUCKLING LOADS FOR EXAMPLE 4, METAL BLADE-STIFFENED PANEL WITH THIN SKIN

Loading				FACTOR							
N_x		N_{xy}									
$\frac{kN}{m}$	$\frac{lbf}{in}$	$\frac{kN}{m}$	$\frac{lbf}{in}$	$F_{d,0}$	$F_{s,0}$	$F_{s,90}$	$F_{d,90}$	$\lambda=L/5$	$\lambda=L/6$	EAL	STAGS
0	0	175.1	1000	0.1761	0.1770	0.6062	0.6031	0.2961	0.3050	0.2767 .305*	0.2773
70.0	400	175.1	1000	.1671	.1679	.5541	.5515	.2428	.2466	.2491	
175.1	1000	175.1	1000	.1548	.1555	.4760	.4739	.1842	.1840	.1881	
350.3	2000	175.1	1000	.1374	.1380	.3695	.3679	.1249	.1227	.1253	
700.5	4000	175.1	1000	.1112	.1115	.2222	.2216	.07197	.06984	.07064	
175.1	1000	0	0	.8611	.9097	.9097	.8611	.3070	.2958	.2965	

*second eigenvalue

Example 5 - Composite Hat-Stiffened Panel

Panel description. - A repeating element of the composite hat-stiffened panel is shown in figure 32. Plate element widths are also shown. The wall construction for each plate element is given in table VIII. Only half the laminate is defined for each plate element because all laminates are symmetric. Plate element numbers are indicated by the circled numbers in figure 32. Values for material properties are the same as those used in example 1 and are given in table II.

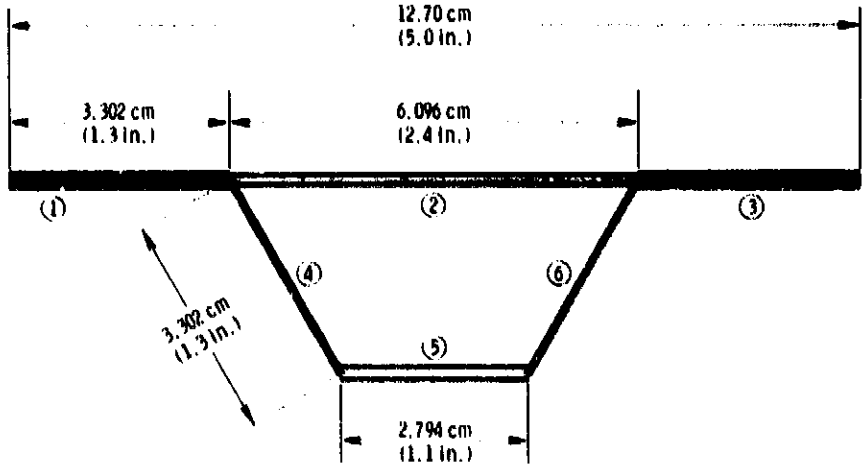

Figure 32.- Repeating element for example 5, composite hat-stiffened panel.

PASCO input and EAL model. - Sample PASCO input for this example is shown in figure 33. The finite element used in the EAL model is the same as that used in the previous models. The finite element grid chosen for the EAL model is shown in figure 34. There are 36 elements used along the length. One finite element is used for plate elements 1, 3, and 5, and two finite elements are used for plate elements 2, 4, and 6. There are 1944 finite elements and 1813 nodes.

```
*****  EXAMPLE 5, COMPOSITE HAT-STIFFENED PANEL  *****
 $CONDAT
 $
 $PANEL
 GRANGE=10,
 IBC=1,
 EL=30,
 B=1.3, 2.4, 1.3, 1.3, 1.1, 1.3,
 T=.010315, .009953, .016955, .025383,
 THET=45, 0, 0, 0,
 KWALL(1,1)= 1,-1,-1,1,2,
 KWALL(1,2)= 1,-1,3,
 KWALL(1,3)= 1,-1,
 KWALL(1,4)= 1,-1,4,
 IWALL=1,2,1,3,4,3,
 HCARD=4,-16,6,60,0,
       4,-14,4,-60,0,
       4,7,14,5,16,
       5,8,1,2,-7,3,
 ICARD=5,1,2,1,-909,0900,
       3,2,5,2,
       3,2,3,14,
       3,3,4,5,
       3,4,5,16,
       3,5,6,3,
       3,6,-909,0900,
 ICREP=6, NOBAY=6,
 MINLAM=30,
 NLAM=1,2,
 SHEAR=.3,
 IP=2,
 NX=1000.,
 $
 $MATER
 E1=19.E6,   E2=1.89E6,  E12=.93E6,  ANU1=.38,  RHO=.0571,
 ALFA1(1)=-.005E-6,     ALFA2(1)=21.8E-6,
 ALLOW(1,1)= 2, .004, -.004, .004, -.004, .01,
 $
```

Figure 33.- Sample PASCO input for example 5, composite hat-stiffened panel.

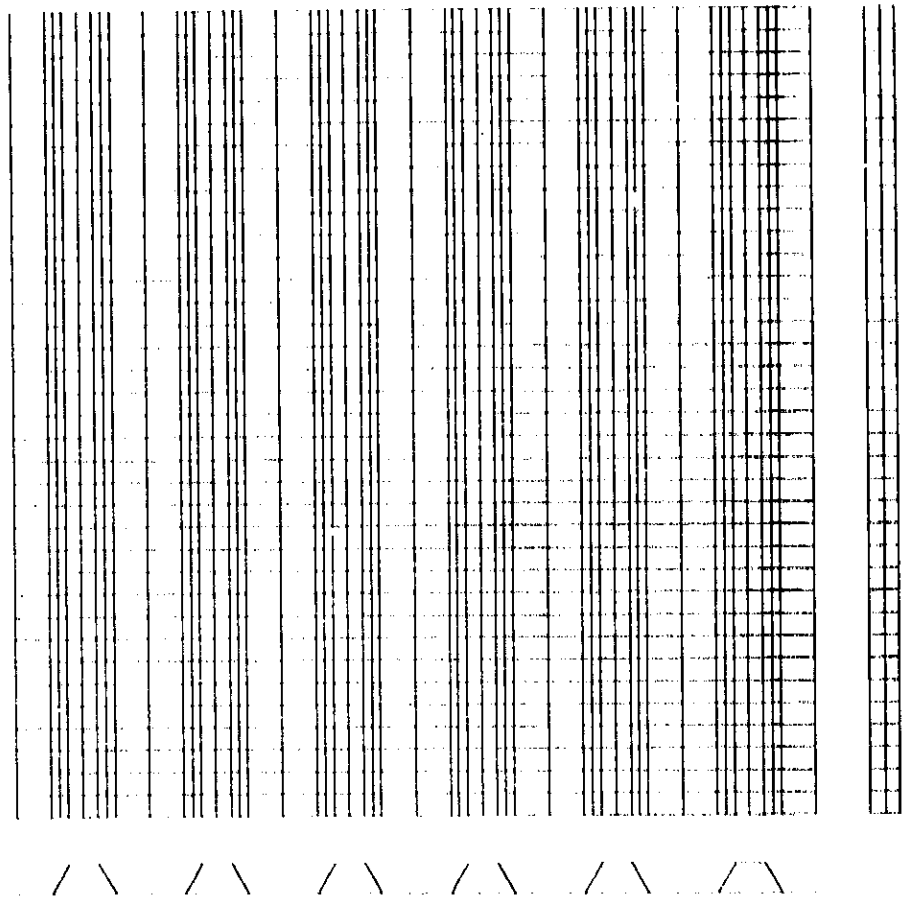

(a) Three views of model.

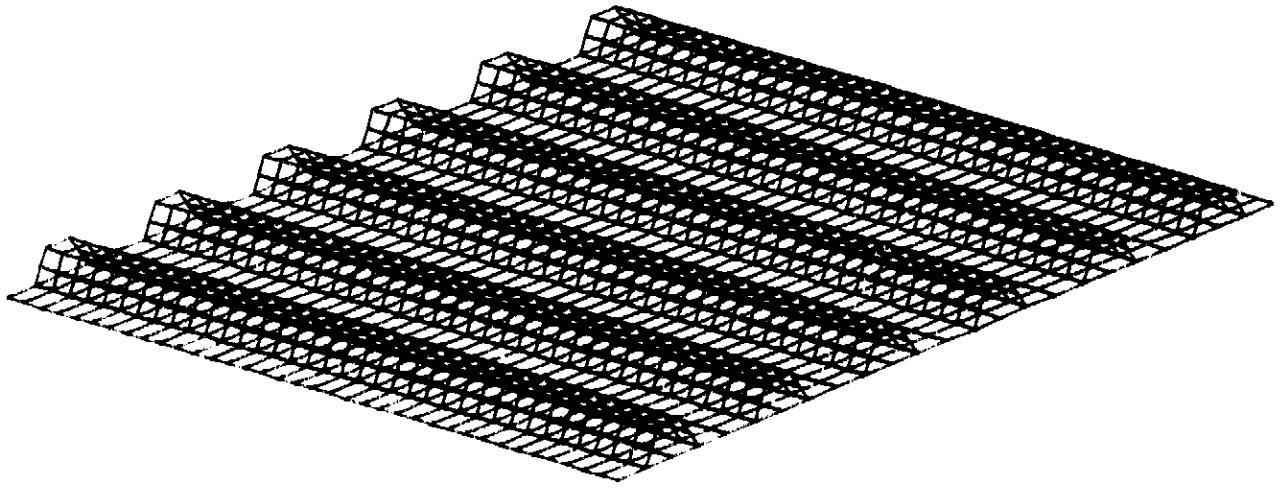

(b) Oblique view.

Figure 34.- EAL finite element model for example 5, composite hat-stiffened panel.

Results. - Buckling results obtained with PASCO and EAL are shown in figure 35. The same general approach used for presenting buckling data in previous examples is used in this example.

For values of N_x less than about 300 kN/m (1700 lb/in), the buckle mode shape for the $F_{s,90}$ solution does not meet the requirement that for $F_{s,90}$ to be valid, the buckling half-wavelength transverse to stiffeners must be at least 2.5 times the stiffener spacing. In the range cited, the buckling half-wavelength is twice the stiffener spacing.

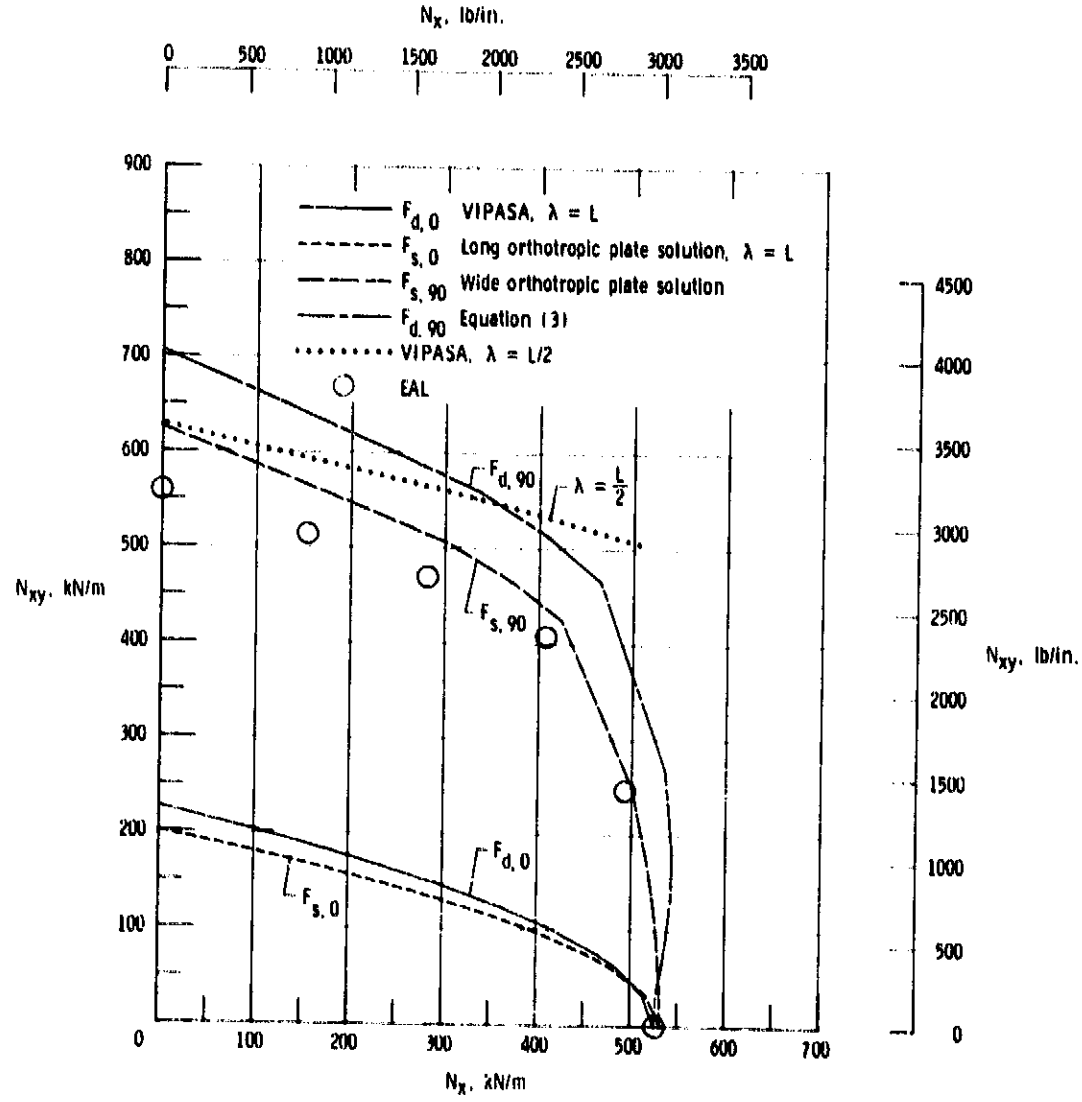

Figure 35.- Buckling load interaction obtained with PASCO and EAL for example 5, composite hat-stiffened panel.

The EAL results (circular symbols) fall below the smeared orthotropic solution $F_{s,90}$ for the entire range of loadings. The EAL result for $N_x = 0$ is an overall mode.

Detailed comparisons of solutions from PASCO and EAL for six loadings are presented in table IX.

The buckle mode shape obtained with EAL for the case $N_x = 0$ is shown in figure 36. The buckle mode shapes obtained with EAL and PASCO for the case $N_{xy} = 0$ are shown in figure 37.

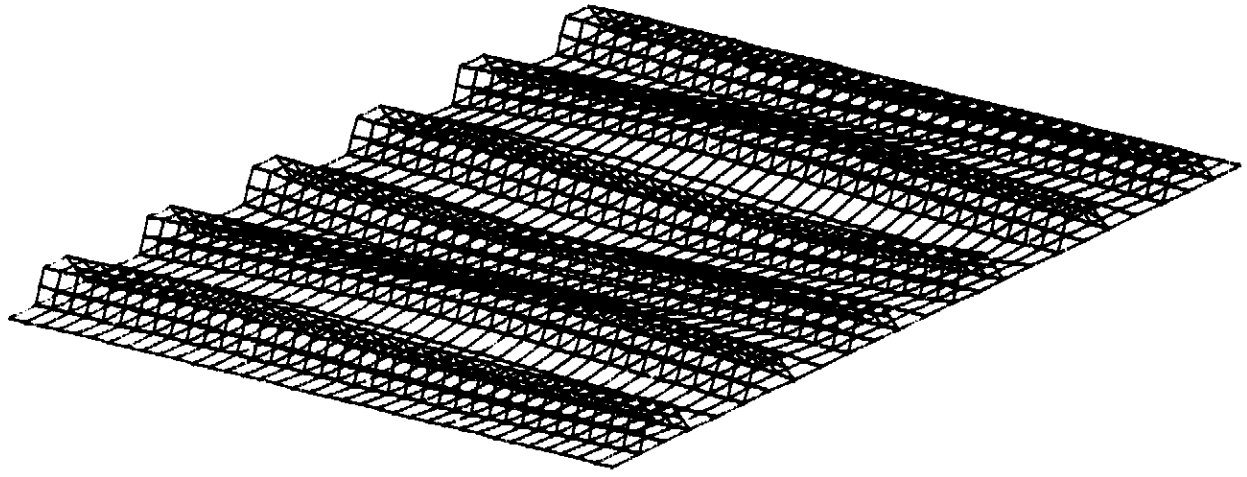

(a) Oblique view.

Figure 36.- Shear buckling mode shape obtained with EAL for example 5, composite hat-stiffened panel.

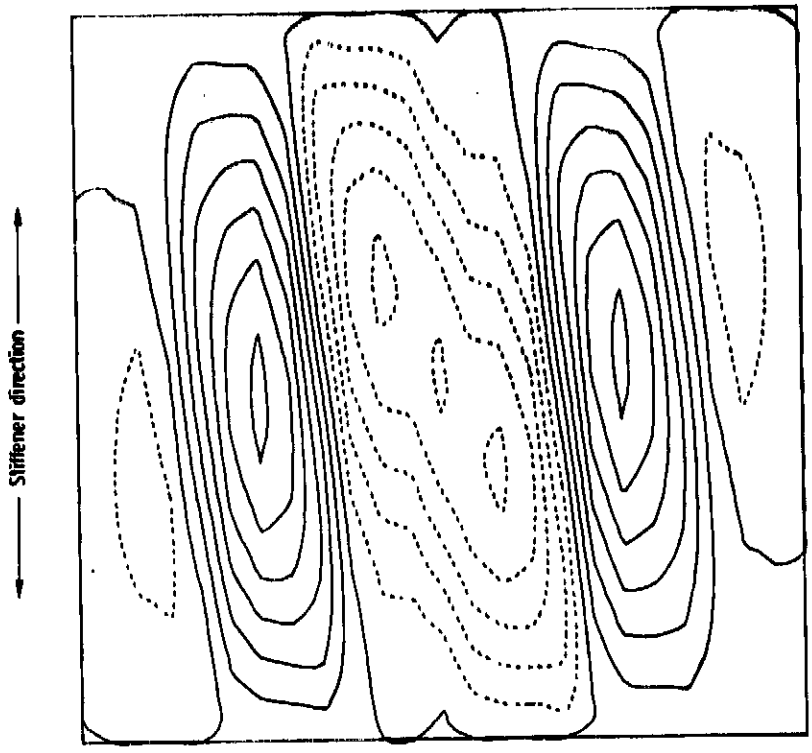

(b) Contour plot.

Figure 36.- Concluded.

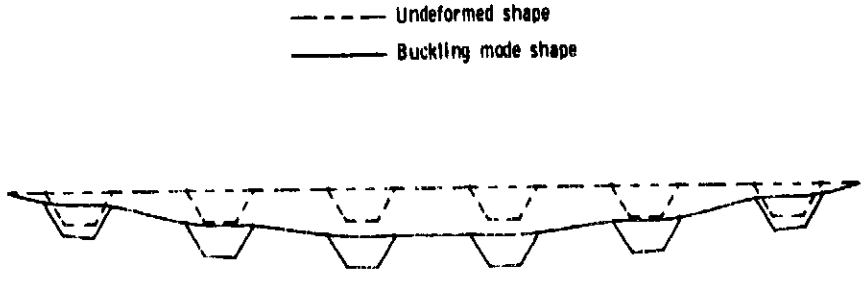

(a) Mode shape obtained with PASCO.

Figure 37.- Buckling mode shape for pure longitudinal compression for example 5, composite hat-stiffened panel.

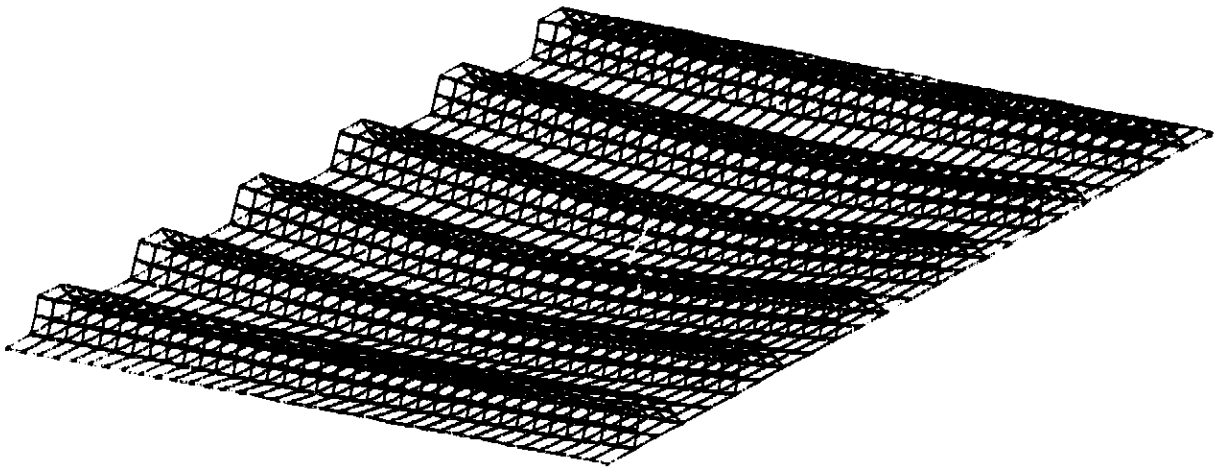

(b) Oblique view of mode shape obtained with EAL.

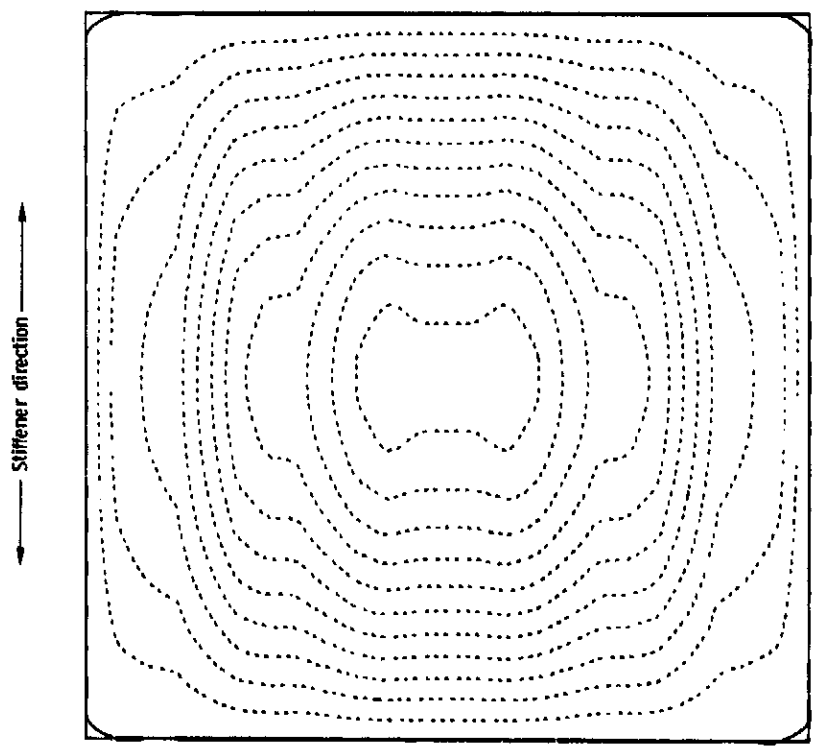

(c) Contour plot of mode shape obtained with EAL.

Figure 37.- Concluded.

TABLE VIII.- WALL CONSTRUCTION FOR EACH PLATE ELEMENT IN EXAMPLE 5, COMPOSITE HAT-STIFFENED PANEL

Layer Number, Starting With Outside Layer	Thickness		Fiber Orientation, Deg
	cm	in	
Plate Elements 1 and 3			
1	0.026200	0.010315	45
2	.026200	.010315	-45
3	.026200	.010315	-45
4	.026200	.010315	45
5	.025281	.009953	0
Plate Element 2			
1	.026200	.010315	45
2	.026200	.010315	-45
3	.043066	.016955	0
Plate Elements 4 and 6			
1	.026200	.010315	45
2	.026200	.010315	-45
Plate Element 5			
1	.026200	.010315	45
2	.026200	.010315	-45
3	.064473	.025383	0

TABLE IX.- BUCKLING LOADS FOR EXAMPLE 5, COMPOSITE HAT-STIFFENED PANEL

Loading				FACTOR					
N_x		N_{xy}							
$\frac{kN}{m}$	$\frac{lbf}{in}$	$\frac{kN}{m}$	$\frac{lbf}{in}$	$F_{d,0}$	$F_{s,0}$	$F_{s,90}$	$F_{d,90}$	$\lambda=L/2$	EAL
0	0	175.1	1000	1.2958	1.1463	3.5698	4.0352	3.6170	3.192
52.5	300	175.1	1000	1.2085	1.0796	3.1933	3.5744	3.3815	2.932
105.1	600	175.1	1000	1.1288	1.0176	2.8822	3.1970	3.1653	2.680
175.1	1000	175.1	1000	1.0331	.9419	2.4229	2.6576	2.9046	2.3268
350.3	2000	175.1	1000	.8389	.7831	1.4265	1.5282	2.3721	1.4062
175.1	1000	0	0	2.9952	3.0351	3.0351	2.9952		3.0042

Example 6 - Composite Corrugated Panel

Panel description. - A repeating element of the composite corrugated panel is shown in figure 38. Element widths are also shown. The wall construction for each plate element is given in table X. Plate element numbers are indicated by the circled numbers in figure 38. Only half the laminate is defined for each plate element because all laminates are symmetric. Values for material properties are the same as those used in example 1 and are given in table II.

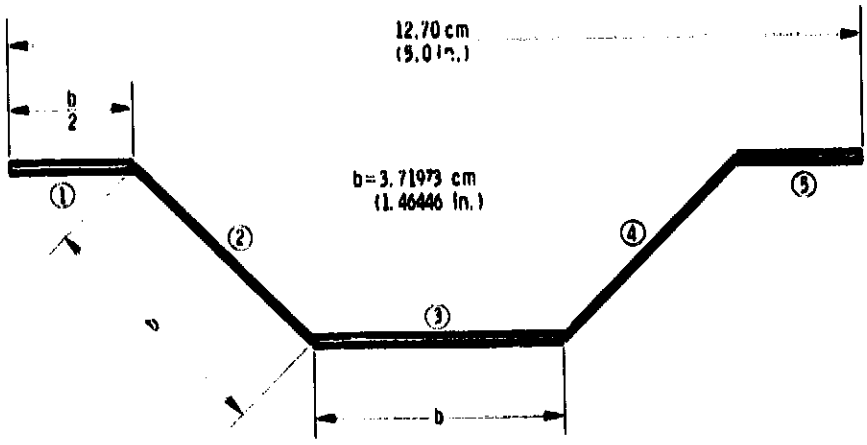

Figure 38.- Repeating element for example 6, composite corrugated panel.

PASCO input and EAL model. - Sample PASCO input for this example is shown in figure 39. The same finite element used in the EAL model of the first example is used in this example. For the EAL finite element model, shown in figure 40, 36 elements are used down the length of the panel, and two elements are used across the width of each plate element.

Results. - Buckling results obtained with PASCO and EAL for this example are shown in figure 41. The EAL results fall above the $F_{s,90}$ curve; therefore, for this case, the adjusted analysis approach is conservative. This conservatism

```
***** EXAMPLE 6, COMPOSITE CORRUGATED PANEL *****
 $CONDAT
 $
 $PANEL
 IBC=1,
 EL=30,
 B= .73223,   1.46446,   1.46446,   1.46446,  .73223,
 T=.005479,  .016836,
 THET=45, 0,
 KWALL(1,1)= 1,-1,-1,1,2,
 KWALL(1,2)= 1,-1,-1,1,
 IWALL=1,2,1,2,1,
 HCARD=4,-6,2,-450, -1,
       4,-7,4,450, -1,
       6,8,1,6,3,7,5,
 ICARD=5,1,2,1,-909,0900,
       3,2,3,6,
       3,3,4,3,
       3,4,5,7,
       3,5,6,5,
       3,6,-909,0900,
 ICREP=6,   NOBAY=6,
 MINLAM=30,
 NLAM=1,2,3,4,
 SHEAR=1,
 IP=2,
 NX=1000.,
 $
 $MATER
 E1=19.E6,   E2=1.89E6,  E12=.93E6,  ANU1=.38,  RHO=.0571,
 ALFA1(1)=-.005E-6,     ALFA2(1)=21.8E-6,
 ALLOW(1,1)= 2, .004, -.004, .004, -.004, .01,
 $
```

Figure 39.- Sample PASCO input for example 6, composite corrugated panel.

is true even though the buckle mode shape for the $F_{s,90}$ solution does not meet the mode shape requirements stated earlier. For the case $N_x = 0$, the buckling half-wavelength transverse to the stiffeners is only 1.2 times the stiffener spacing. Results from the other examples suggest that a buckle half-wavelength of only 1.2 times the stiffener spacing would cause $F_{s,90}$ to be very unconservative. Detailed comparisons of results from PASCO and EAL for six loadings are presented in table XI.

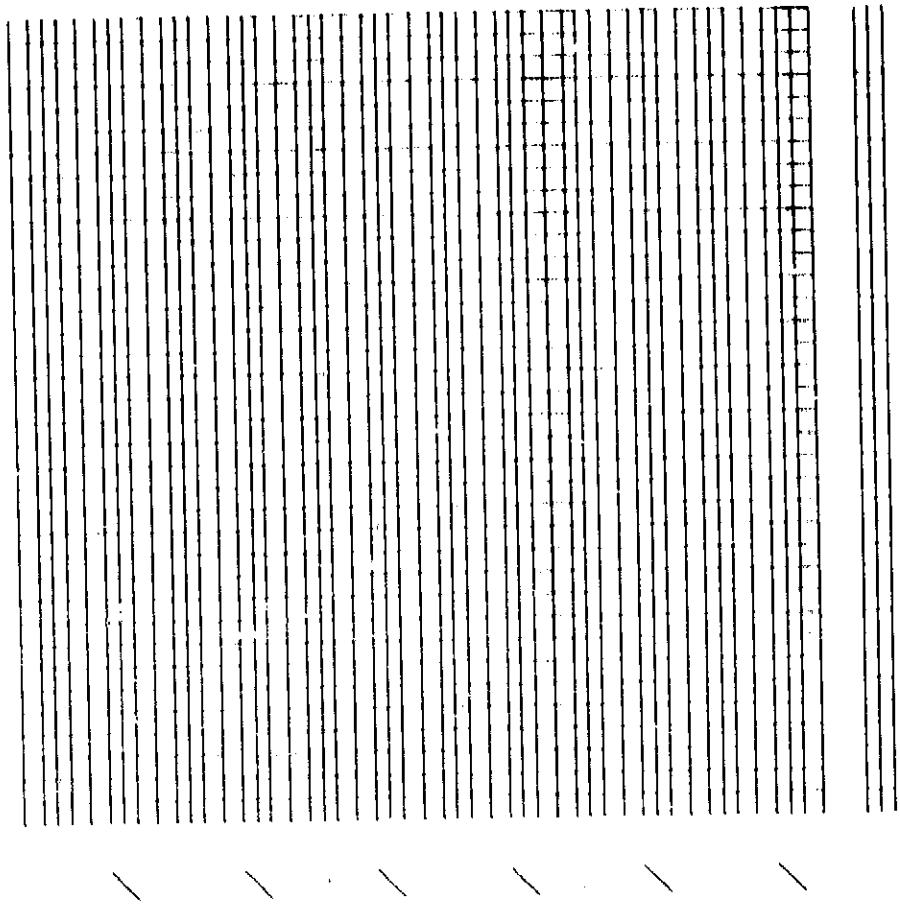

(a) Three views of model.

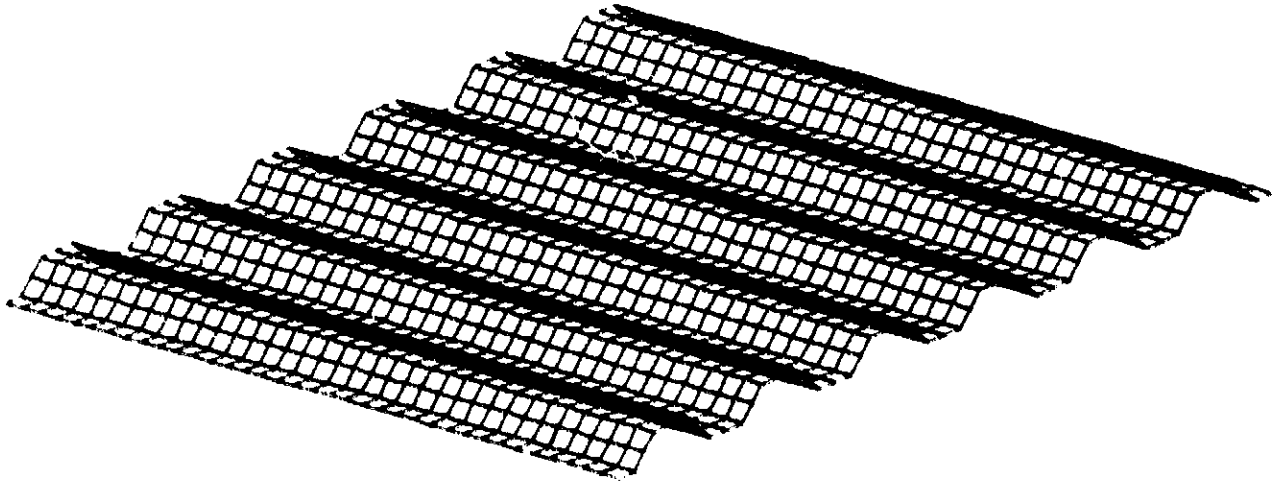

(b) Oblique view of model.

Figure 40.- EAL finite element model for example 6, composite corrugated panel.

The buckle mode shape for the pure shear case, figure 42, shows that buckling is limited to the area near the lateral edges. It is possible that this mode is associated with the inplane boundary conditions (fig. 10) on the lateral edges and with the low value of the extensional stiffness of the panel in the y-direction. The buckle mode shapes obtained with EAL and PASCO for the case $N_{xy} = 0$ are shown in figure 43.

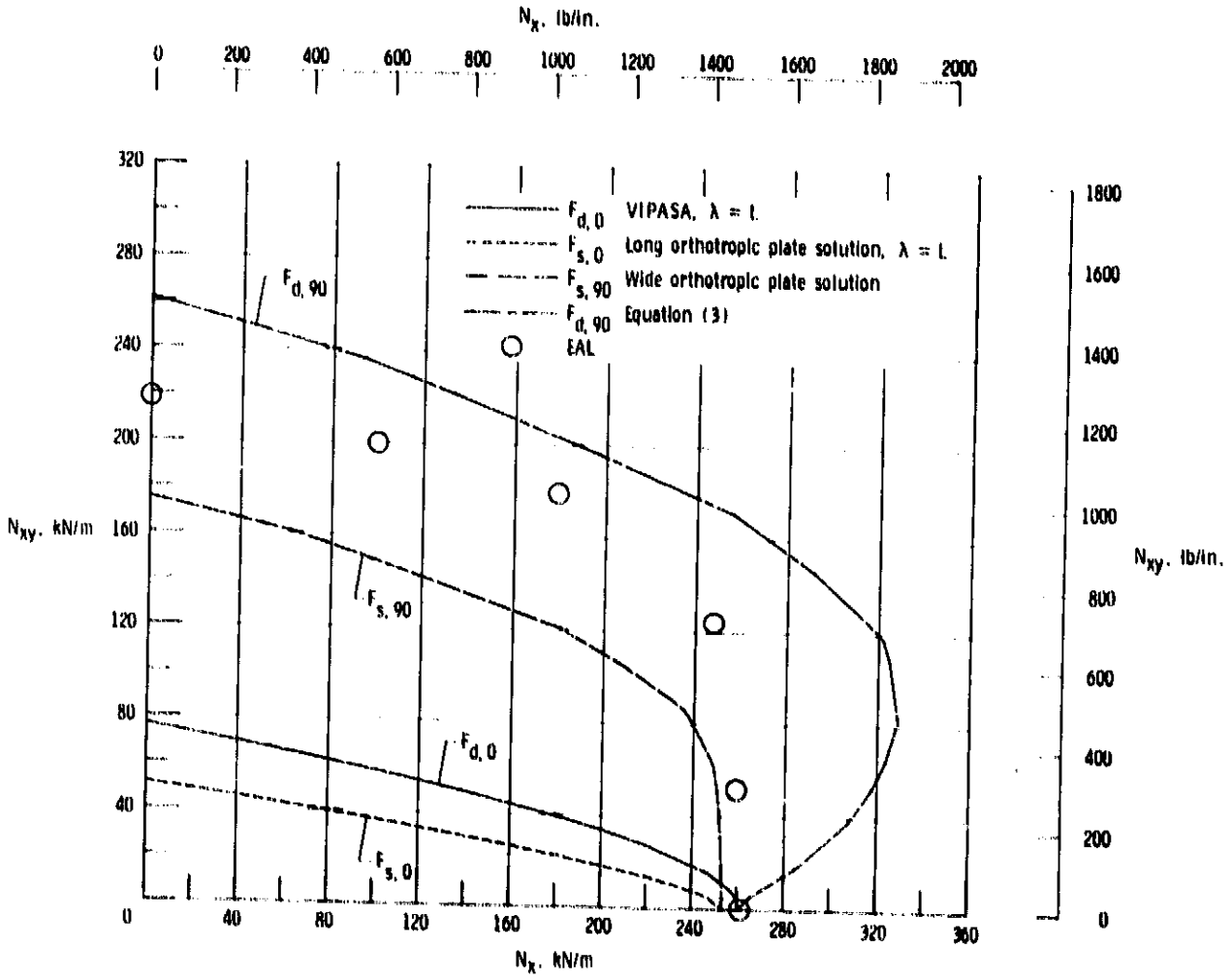

Figure 41.- Buckling load interaction obtained with PASCO and EAL for example 6, composite corrugated panel.

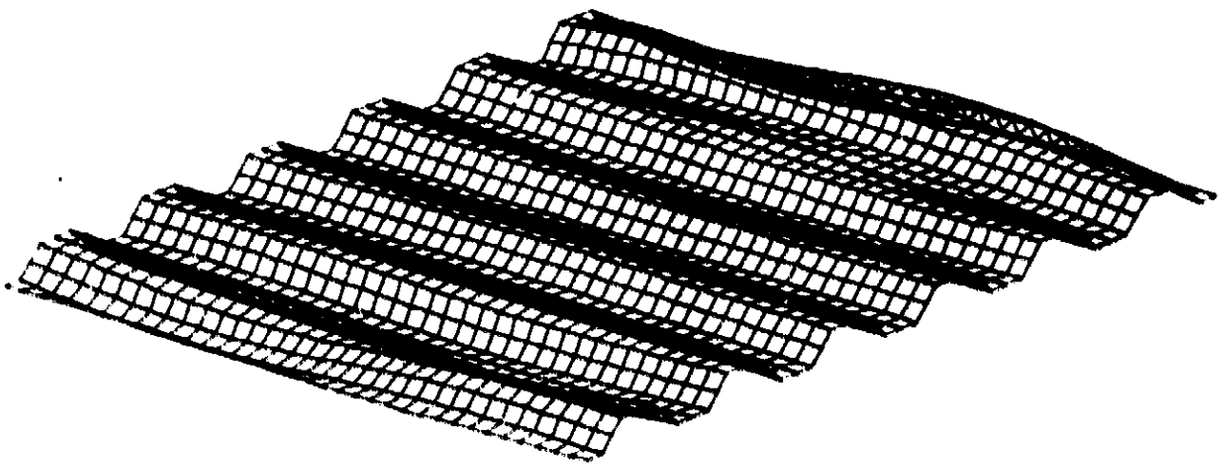

Figure 42.- Shear buckling mode shape obtained with EAL for example 6, composite corrugated panel.

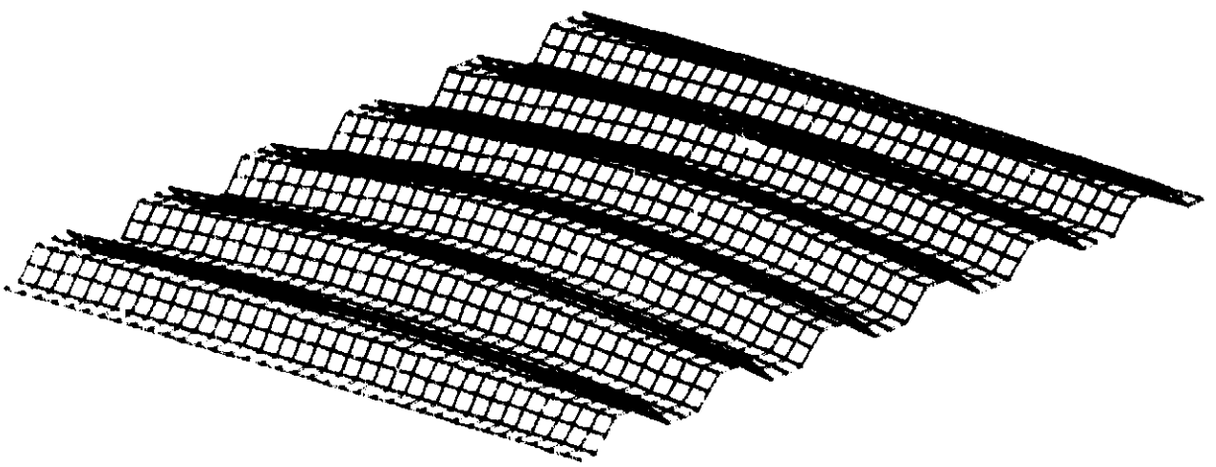

(a) Mode shape obtained with EAL.

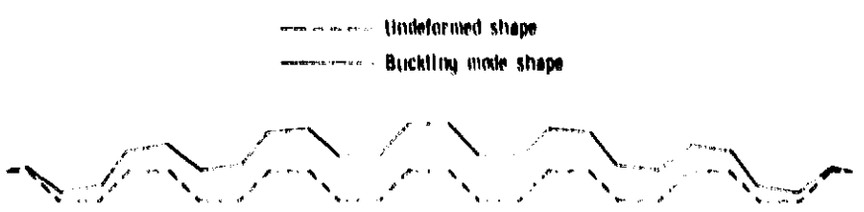

(b) Mode shape obtained with PASCO.

Figure 43.- Buckling mode shape for pure longitudinal compression for example 6, composite corrugated panel.

TABLE X.- WALL CONSTRUCTION FOR EACH PLATE ELEMENT IN EXAMPLE 6, COMPOSITE CORRUGATED PANEL

Layer Number, Starting With Outside Layer	Thickness		Fiber Orientation, Degrees
	cm	in	
Plate Elements 1, 3, and 5			
1	0.013917	0.005479	45
2	.013917	.005479	-45
3	.013917	.005479	-45
4	.013917	.005479	45
5	.042763	.016836	0
Plate Elements 2 and 4			
1	.013917	.005479	45
2	.013917	.005479	-45
3	.013917	.005479	-45
4	.013917	.005479	45

TABLE XI.- BUCKLING LOADS FOR EXAMPLE 6, COMPOSITE CORRUGATED PANEL

LOADING				FACTOR				
N_x		N_{xy}						
$\frac{kN}{m}$	$\frac{lbf}{in}$	$\frac{kN}{m}$	$\frac{lbf}{in}$	$F_{d,0}$	$F_{s,0}$	$F_{s,90}$	$F_{d,90}$	EAL
0	0	175.1	1000	0.4396	0.2937	1.0011	1.4986	1.248
87.6	500	175.1	1000	.4032	.2742	.8894	1.3077	1.1395
175.1	1000	175.1	1000	.3711	.2568	.7780	1.1242	1.0223
350.3	2000	175.1	1000	.3176	.2270	.5971	.8352	.7077
875.6	5000	175.1	1000	.2138	.1654	.2865	.3703	.2958
175.1	1000	0	0	1.4897	1.4462	1.4462	1.4897	1.4918

DISCUSSION OF RESULTS

The basic conclusion that can be drawn from these calculations is that a buckling solution based on smeared orthotropic stiffnesses should be used only with caution. In most of the calculations, the smeared orthotropic solution $F_{s,90}$ overestimated the overall buckling load. Two factors appeared to contribute to the error: (1) smeared orthotropic buckling modes with half-wavelength transverse to the stiffeners less than 2.5 times the stiffener spacing, and (2) shorter wavelength buckling modes, such as $\lambda = L/2$, which fall below or in the vicinity of the $F_{s,90}$ curve. In all cases, the finite element solution for overall buckling falls between the VIPASA solutions for $\lambda = L$ and $\lambda = L/2$. A solution approach for overall shear buckling that assumes the buckling mode to be a combination of the first few VIPASA modes is being studied. A special procedure is needed to combine these modes in such a way that the boundary conditions at the panel ends are satisfied.

Based on these results, the following rough guidelines for using the adjusted analysis are recommended. If the buckling mode shape for the smeared orthotropic solution $F_{s,90}$ has a half-wavelength transverse to the stiffeners that is less than 1.5 times the stiffener spacing, then accept no increase in buckling load above the standard VIPASA solution $F_{d,0}$. If the buckling half-wavelength transverse to the stiffeners is greater than 2.5 times the stiffener spacing, then accept no more than 75 percent of the increase above the standard VIPASA solution. Make additional adjustments if local modes are present. These guidelines are conservative for the six panels considered, but greatly underestimate the load carrying ability of the corrugated panel. Finally, for structural sizing applicatons it is recommended that the adjusted analysis not be used. The resulting panels will be light-weight and conservatively designed.

CONCLUDING REMARKS

PASCO's buckling analysis (VIPASA) is reviewed, and an important shortcoming of that analysis--underestimation of long-wavelength shear buckling loads--is explained. An alternate overall shear buckling analysis based on smeared orthotropic stiffnesses is presented. The alternate analysis is referred to as the adjusted analysis.

Buckling calculations were carried out with PASCO, EAL, and STAGS computer programs to study the conservatism in the VIPASA solution and to evaluate the adjusted analysis. Six stiffened panels were studied: two composite blade-stiffened panels, two metal blade-stiffend panels, one composite hat-stiffened panel, and one composite corrugated panel. The loadings were combinations of longitudinal compression and shear. It is shown that the adjusted analysis may be unconservative.

The adjusted analysis for overall shear buckling is an engineering approximation and engineering judgment should be used in its application. Rough guidelines that might be used are as follows. If the buckling mode shape for the smeared orthotropic solution $F_{s,90}$ (part of the adjusted shear analysis) has a half-wavelength transverse to the stiffeners that is less than 1.5 times the stiffeners spacing, then accept no increase in buckling load above the standard VIPASA solution $F_{d,90}$. If the buckling half-wavelength transverse to the stiffeners is greater than 2.5 times the stiffener spacing, then accept no more than 75 percent of the increase above the standard VIPASA solution. It is recommended that the adjusted analysis not be used for structural sizing applications.

REFERENCES

1. Wittrick, W. H.; and Williams, F. W.: Buckling and Vibration of Anisotropic or Isotropic Plate Assemblies Under Combined Loadings, Int. J. Mech. Sci., Vol. 16, No. 4, Apr. 1974, pp. 209-239.

2. Anderson, Melvin S.; Hennessy, Katherine W.; and Heard, Walter L., Jr.: Addendum to Users Guide to VIPASA (Vibration and Instability of Plate Assemblies Including Shear and Anisotropy). NASA TM X-73914, 1976.

3. Williams, F. W.; and Anderson, M. E.: User's Guide to VIPASA (Vibration and Instability of Plate Assemblies Including Shear and Anisotropy). Department of Civil Engineering, University of Birmingham (England), January 1973.

4. Viswanathan, A. V.; and Tamekuni, M.: Elastic Buckling Analysis for Composite Stiffened Panels and Other Structures Subjected to Biaxial Inplane Loads. NASA CR-2216, September 1973.

5. Stroud, W. Jefferson; and Agranoff, Nancy: Minimum-Mass Design of Filamentary Composite Panels Under Combined Loads: Design Procedure Based on Simplified Buckling Equations. NASA TN D-8257, October 1976.

6. EISI/SPAR Reference Manual, System Level 103, Engineering Information Systems Inc., San Jose, CA, January 1979.

7. Whetstone, W. D.: Engineering Data Management and Structure of Program Functions in New Techniques in Structural Analysis by Computer (Compiled by R. J. Melosh and M. Salana) ASCE Preprint 3601, ASCE Convention and Exposition, Boston, Massachusetts, 1979.

8. Almroth, B. P.; and Brogan, F. A.: The STAGS Computer Code. NASA CR-2950, 1978.

9. Almroth, B. P.; Brogan, F. A.; and Stanley, G. M.: Structural Analysis of General Shells, Volume II: User Instructions for STAGSC-1. NASA CR 165671, January 1981.

10. Anderson, Melvin S.; and Stroud, W. Jefferson: A General Panel Sizing Computer Code and Its Application to Composite Structural Panels. AIAA J., Vol. 17, No. 8, August 1979, pp. 892-897.

11. Stroud, W. Jefferson; and Anderson, Melvin S.: PASCO: Structural Panel Analysis and Sizing Code, Capability and Analytical Foundations. NASA TM 80181, 1981. (Supersedes NASA TM 80181, 1980)

12. Anderson, Melvin S.; Stroud, W. Jefferson; Durling, Barbara J.; and Hennessy, Katherine W.: PASCO: Structural Panel Analysis and Sizing Code, Users Manual. NASA TM 80182, 1981. (Supersedes NASA TM 80182, 1980)

13. Stein, Manuel; and Fralich, Robert W.: Critical Shear Stress of Infinitely Long, Simply Supported Plate with Transverse Stiffeners, NACA TN 1851, 1949.

14. Gallagher, Richard H.: Finite Element Analysis, Fundamentals. Prentice-Hall, 1975.